



## A comparison of heterogeneous ice nucleation parameterizations using a parcel model framework

Trude Eidhammer,<sup>1,2</sup> Paul J. DeMott,<sup>1</sup> and Sonia M. Kreidenweis<sup>1</sup>

Received 3 September 2008; revised 12 January 2009; accepted 22 January 2009; published 17 March 2009.

[1] A liquid-phase Lagrangian parcel model was expanded to include nucleation and growth of ice crystals. Intercomparisons between three heterogeneous ice nucleation parameterizations that link aerosol type and number to ice crystal concentration were conducted. Results indicate large differences in the prediction of ice formation in modestly supercooled clouds and in the susceptibility of cirrus to heterogeneous ice nucleation for the same assumed aerosol distribution. Only one parameterization has an observational constraint that limits the maximum ice crystal number concentrations to be a fraction of the total number concentrations of potential ice-nucleating particles (typically, all insoluble particles larger than about 0.1  $\mu\text{m}$ ). The constrained parameterization compares well with most ice nucleation measurements. The unconstrained parameterizations are capable of predicting several orders of magnitude higher ice crystal concentrations than the constrained parameterization for the same parcel-forcing conditions. Ice crystal concentrations in the unconstrained parameterizations are controlled by the total number concentration of potential ice-nucleating particles and, importantly, negative feedback on ice supersaturation. This feedback control often masks the large discrepancy that exists between predicted ice crystal number concentrations and the maximum number concentrations that can be attributed to atmospheric ice nuclei based on our current understanding of the latter. It also permits unrealistic conclusions regarding the role of certain aerosols as ice nuclei. It is recommended that a constraint on ice crystal number concentrations, related to number concentrations of relevant aerosol particles, should be included in ice nucleation parameterizations used in cloud to global-scale models.

**Citation:** Eidhammer, T., P. J. DeMott, and S. M. Kreidenweis (2009), A comparison of heterogeneous ice nucleation parameterizations using a parcel model framework, *J. Geophys. Res.*, 114, D06202, doi:10.1029/2008JD011095.

### 1. Introduction

[2] Ice crystals in the atmosphere form via several different pathways involving homogeneous and heterogeneous ice nucleation. While homogeneous freezing occurs in liquid solutions, heterogeneous nucleation occurs on a solid particle (ice nuclei, IN). Heterogeneous nucleation mechanisms include deposition, condensation freezing, immersion freezing and contact freezing [see *Vali*, 1985]. Only a few types of solid particles in the atmosphere serve as IN, and the number fraction of the population of solid particles that are IN varies greatly with particle type, temperature, and supersaturation with respect to ice.

[3] The inclusion of heterogeneous ice nucleation parameterizations in general circulation models and cloud resolving models often does not consider the different types of IN

and the variation of IN number concentrations throughout the atmosphere. These models often use diagnostic parameterizations that predict IN number concentration only as a function of temperature [*Cooper*, 1986; *Fletcher*, 1962] or as a function of ice supersaturation [*Meyers et al.*, 1992]. Such parameterizations do not account for the variability of IN number concentration in space and time in the atmosphere and they are often applied outside the temperature or supersaturation range of the measurements on which they were based. For example, the *Meyers et al.* formulation will overpredict ice crystal concentrations when the number concentration of particles that can act as IN is low, as shown by *Prenni et al.* [2007b] in Arctic conditions. The Fletcher parameterization will typically underpredict ice crystal concentrations at warm temperatures but overpredict at lower temperatures [*Meyers et al.*, 1992].

[4] Increased knowledge of ice nucleation from field and laboratory studies, and the increased capability to include more detailed aerosol treatment in models, has led to the development of several different model representations of heterogeneous ice nucleation that take into account that different types of aerosols can act as IN with different nucleating efficiencies [*Diehl and Wurzler*, 2004; *Kärcher*

<sup>1</sup>Department of Atmospheric Science, Colorado State University, Fort Collins, Colorado, USA.

<sup>2</sup>Now at RAL/TIIMES, National Center for Atmospheric Research, Boulder, Colorado, USA.

and Lohmann, 2003; Khvorostyanov and Curry, 2004; Liu and Penner, 2005; Phillips et al., 2008]. These parameterizations can therefore be used to study aerosol-cloud effects by individual IN types [Diehl et al., 2006, 2007; Kärcher et al., 2006, 2007; Liu et al., 2007; Lohmann and Diehl, 2006]. However, the abovementioned parameterizations are based on different “pathways of development” (i.e., from classical nucleation theory, laboratory studies and field work), and they have also been designed to depend on different aerosol parameters. Further, they have various, or no, direct constraints on the maximum number of ice crystals that can be formed in relation to the concentration of insoluble aerosols that potentially can serve as IN. The predicted ice crystal number concentrations and conditions required for the onset of ice nucleation might therefore vary greatly between the different parameterizations.

[5] Simple comparisons between several heterogeneous ice nucleation parameterizations, assuming constant water saturation, were conducted by Phillips et al. [2008]. Here, we expand on those comparisons, describing and applying an adiabatic parcel model to conduct intercomparison studies between three heterogeneous ice nucleation parameterizations. The parcel model computes the time-dependent water supersaturation, which responds to both external forcing and to uptake by drops and crystals. We focus these studies on heterogeneous ice nucleation in the immersion or condensation freezing modes. We explore the behavior and implications of the parameterizations in mixed-phase and cirrus cloud parcel simulations, then address their consistency with existing field measurements of ice nucleation and discuss how inconsistencies could lead to unrealistic predictions when the parameterizations are applied in cloud and climate simulations.

## 2. Parcel Model

[6] The comparison studies of heterogeneous ice nucleation parameterizations are conducted with a Lagrangian parcel model, developed by Feingold and Heymsfield [1992]. The original parcel model calculates droplet growth by condensation in an adiabatic updraft, or along trajectories, with prescribed atmospheric parameters. The initial dry aerosol is binned into a selected number of sizes, and the growth of each size bin is computed (the Lagrangian approach for drop size histories). The set of conservation equations is solved using the Variable-coefficient Ordinary Differential Equation (VODE) solver [Brown et al., 1989]. This parcel model has been applied in several studies, including the studies of Feingold et al. [1998], Feingold and Kreidenweis [2000], Ervens et al. [2005], and Koehler et al. [2006]. We have modified the original parcel model as follows: we replaced the existing solution thermodynamics module, used for drop activation and condensational growth, with a recent simpler parameterization by Petters and Kreidenweis [2007]; we modified the calculation of saturation ratio for the case of an adiabatic parcel; and we added descriptions of nucleation of ice and of ice crystal growth. These changes are described in more detail in Appendix A, and discussed only briefly here. The set of ordinary differential equations for calculating changes in temperature, pressure, saturation ratio, liquid water con-

tent (from droplet growth equations) and air density with time are also given in Appendix A1.

[7] Homogeneous ice nucleation follows the parameterization developed by Koop et al. [2000], while heterogeneous ice nucleation follows parameterizations that are described in section 3. Diffusional growth of ice crystals is calculated as in equation (13)–(76) of Pruppacher and Klett [1997], assuming spherical particles, a deposition coefficient of 1.0 and that the ice grows with the bulk ice density. An aerosol particle or cloud drop that freezes must be removed from its Lagrangian bin and put into a separate category, because the growth equations for particles/drop and ice crystals are different. Rather than spawning a new bin size for each newly formed ice crystal at each time step, we follow a hybrid Lagrangian/Eulerian framework based on principles described by Cooper et al. [1997]. The binning method for ice is described in Appendix A2.

[8] The external time step at which output is recorded in the parcel model is  $50 \text{ cm w}^{-1}$ , where  $w$  is the vertical velocity in  $\text{cm s}^{-1}$ . We also use this time step to compute new ice formation and to reorganize the crystal bin structure. The calculation of particle growth by condensation and deposition, however, has a higher internal time resolution set up by the VODE procedure. Sensitivity studies show little variation in liquid water content (LWC), ice water content (IWC), and ice crystal number concentration by using a higher external time resolution for the ice formation/crystal bin reorganization processes than  $50 \text{ cm w}^{-1}$ , where  $w$  is the vertical velocity assumed in the simulation.

[9] To test the representation of ice formation in our revised parcel model, we conducted simulations that followed the 6 different initial conditions used in the homogeneous nucleation cases of the “Cirrus Parcel Model Comparison Project” (CPMCP) [Lin et al., 2002]. Our predicted ice crystal number concentrations compared well with the results from the model developed by Kärcher [2003] (note that for this comparison we used the same deposition coefficients as participants in CPMCP), which also used the approach of Koop et al. [2000] for parameterizing homogeneous freezing nucleation.

## 3. Heterogeneous Ice Nucleation Parameterizations

[10] We selected three specific parameterizations of heterogeneous ice nucleation for comparison because each links ice initiation to aerosol properties and number concentrations, as distinguished from other parameterizations that use for example supersaturation alone as the trigger for ice formation [e.g., Meyers et al., 1992]. The bases for the development of these schemes are from classical heterogeneous nucleation theory [Khvorostyanov and Curry, 2000, 2004], laboratory studies of droplet freezing [Diehl and Wurzler, 2004], and field studies constrained by laboratory cloud chamber studies [Phillips et al., 2008]. The equations pertaining to each parameterization are listed in Appendix B.

[11] The Khvorostyanov and Curry [2004] scheme (hereafter called KC04) computes the theoretical ice nucleation rate (or rate of heterogeneous germ formation) for aqueous solution drops. It is assumed that the solution drop was formed from a mixed particle containing soluble and insol-

uble material, and that the insoluble material acts as an IN. This nucleation scheme accounts for condensation and immersion freezing, and KC04 adopted the term “deliquescent-heterogeneous freezing” to separately distinguish freezing of deliquesced particles at subsaturated conditions relative to water [DeMott, 2002]. The explicit treatment of KC04 appears to reconcile classical theory with the effective freezing temperature [e.g., DeMott et al., 1997] and water-activity-dependent freezing [Koop et al., 2000] parameterizations that capture “nonideal” impacts of dissolved solute on freezing. The KC04 scheme gives the ice nucleation rate as a function of both temperature and water supersaturation. In addition, the nucleation rate is also dependent on the size and surface properties of the insoluble material. The surface properties are accounted for by the contact angle ( $\theta$ ), relative area of active sites ( $\alpha$ ), and elastic strain ( $\varepsilon$ ). The idea of a relative area of active sites was first introduced in the classical heterogeneous nucleation theory by Fletcher [1969] and is defined as a relative area where  $\theta = 0$ . The effect of elastic strain, which is produced by crystallographic misfit between ice and the nucleating substrate and therefore decreases the nucleability of the insoluble surface, was introduced by Turnbull and Vonnegut [1952]. Different types of IN and their freezing abilities are assumed in KC04 by varying these surface properties. For example, lower contact angles imply freezing at warmer temperatures. Measurements suggest that quartz particles have contact angles of  $43\text{--}50^\circ$ , surface soil:  $65\text{--}69^\circ$  [Pruppacher and Klett, 1997, Table 5.2] and soot:  $55\text{--}63^\circ$  [Kärcher et al., 1996]. The KC04 scheme has been used in cloud resolving modeling studies by Khvorostyanov et al. [2006], Morrison and Pinto [2006] and Sassen and Khvorostyanov [2007], among others.

[12] Diehl and Wurzler [2004] (hereafter called DW04) proposed a parameterization for heterogeneous ice nucleation through the immersion freezing mode. This parameterization assumes the singular or deterministic freezing hypothesis: that nucleation of an individual particle takes place at or below a defined critical temperature [Langham and Mason, 1958; Vali, 1994]. The singular hypothesis assumes that freezing is time-independent. Several observations seem to support the singular hypotheses [Cooper and Vali, 1981; DeMott, 1990; Marcolli et al., 2007; Möhler et al., 2006; Shaw et al., 2005; Vali, 1994] or modified singular hypotheses [Vali, 2008]. The DW04 parameterization gives a semi-empirical equation for the freezing of drops in the immersion mode based on laboratory freezing experiments of 7 different IN types (soot particles from kerosene; three mineral particle types: kaolinite, montmorillonite and illite; and three biological particles: pollen, leaf litter and bacteria). The freezing of a drop containing a specific insoluble particle type is based on the median freezing temperature of an observed monodisperse drop population. As Diehl and Wurzler note, a disadvantage of using the median freezing temperature is that early onset freezing of a few droplets is not captured, which in some cases can be important. For example, the first freezing events may prevent the occurrence of additional freezing nucleation when considering the impact of the Wegener-Bergeron-Findeisen (WBF) process [Bergeron, 1935; Findeisen, 1938; Wegener, 1911] or negative feedback on ice supersaturation [Khvorostyanov and Curry, 2005]. From the median freezing temperature of the seven specific compounds included in their study, DW04 defined a constant that

represents the efficiency of ice nucleation in the immersion mode per unit volume of liquid, where the liquid has an insoluble particle immersed in it. It is assumed that the drop freezing is independent of the cooling rate and of the number density of insoluble particles in the droplets. A freezing point depression due to salts in the droplets is also accounted for empirically. Thus the freezing of droplets according to DW04 is a function of composition of insoluble material type, droplet volume, and concentration of soluble material, but it is not a function of the size of the particle that can serve as IN. The DW04 parameterization has been used in parcel model sensitivity studies by Diehl et al. [2006, 2007], and in global climate modeling simulations by Lohmann and Diehl [2006] and Lohmann et al. [2007].

[13] The parameterization developed by Phillips et al. [2008] (hereafter called PDA08) is empirical and based on field measurements of aerosol and IN from the Ice Nuclei Spectroscopy (INSPECT) campaigns [DeMott et al., 2003a; Richardson et al., 2007], but constrained by laboratory measurements (see references within). As for the DW04 parameterization, the singular hypothesis is also assumed for the PDA08 parameterization and it predicts the total number of IN as a small subpopulation of the aerosol population at a given temperature and ice supersaturation. It uses the observation that there is a relationship between total surface area of a given distribution of particles larger than  $\sim 0.10\ \mu\text{m}$  in diameter, and the number of IN in the same sample, as also expected on the basis of classical theory. Therefore the number of IN predicted with the PDA08 parameterization is a strong function of the number concentration of particles  $>0.1\ \mu\text{m}$ . Further, the number fraction of aerosol active as IN is “predetermined” in the parameterization itself through temperature and supersaturation control (see Appendix B). Variations in the number concentrations, or total surface area, in the population that can serve as IN are scaled or otherwise constrained according to the field measurements, thus allowing for high IN concentration in high aerosol loadings and the opposite for low aerosol loadings. Three different IN types are included in the PDA08 parameterization, dust, soot and organic carbon, each with different activation properties. The PDA08 parameterization is assumed to account for deposition, condensation freezing and immersion freezing since the ice nucleation data are nonspecific to these particular mechanisms.

#### 4. Heterogeneous Ice Nucleation Simulations in the Immersion- and Condensation-Freezing Modes in Mixed Phased Regime

[14] We used the parcel model to compare the three abovementioned heterogeneous ice nucleation parameterizations. In doing so, we must acknowledge that parcel models are in many cases too simple for real cloud modeling studies. There are no dynamical or radiative feedbacks included, and precipitation and sedimentation are difficult to account for. Only for cloud systems where precipitation and mixing can be assumed to be negligible, such as for example the initiation of ice formation in lenticular clouds of limited vertical extent, can parcel models be used to attempt to model a cloud system. However, parcel models are appropriate when the focus of the study is microphysical processes or sensitivity

studies. Further, most modern measurements of atmospheric ice nucleation do not possess the same limitations imposed by real clouds processes, in particular, the detection of IN is not limited by depletion of supersaturation in the instrument. Therefore the robustness of parameterizations against field measurements is best checked in a framework that allows for clear resolution of the impacts of nucleation itself versus processes that generate and deplete water vapor.

[15] Our first sets of simulations are for initial temperatures too warm to support homogeneous nucleation, and examine the differences in ice crystal number concentrations produced by the three selected parameterizations under these conditions. The simulations were initialized with two different temperatures (10 and  $-14^{\circ}\text{C}$ ). In the  $10^{\circ}\text{C}$  simulations, constant updraft velocities of 50 and  $500\text{ cm s}^{-1}$  were assumed, while in the  $-14^{\circ}\text{C}$  simulations updraft velocities of 5 and  $50\text{ cm s}^{-1}$  were assumed. The initial pressure is always 800 hPa. We follow several published parcel model sensitivity studies by assuming the IN to be contained in an aerosol that is an internal mixture of soluble and insoluble material [e.g., *DeMott et al.*, 1997; *DeMott et al.*, 1998; *Diehl et al.*, 2006; *Khvorostyanov and Curry*, 2005]. We assume the volume fraction of soluble material in each particle is 10%. We conducted a few test simulations with volume fraction of 50%, but for the purpose of this paper, the difference was negligible.

[16] For all simulations, we assume the aerosol distribution is bimodal, with one mode containing only soluble material and the other containing the internal mixture described above. The mode containing only soluble material is assumed to be ammonium sulfate with hygroscopicity  $\kappa_s = 0.6$  [*Petters and Kreidenweis*, 2007], geometric median radius  $\mu_g = 0.02\text{ }\mu\text{m}$ , and geometric standard deviation  $\sigma_g = 2.3$ . In the following simulations, the number concentration in the soluble-only mode is assumed to be  $200\text{ cm}^{-3}$  which is a reasonable choice for representing either the marine boundary layer environment or the free troposphere.

[17] The second mode contains the internally mixed aerosols that can act as both IN and CCN, and we assume these particles to be larger than those in the soluble-only mode, as ice crystal and snow residuals indicate that the IN sizes are typically larger than  $0.1\text{ }\mu\text{m}$  [e.g., *Prenni et al.*, 2007a; *Pruppacher and Klett*, 1997]. We also chose different size distributions depending on the type of insoluble material, as suggested by *Phillips et al.* [2008]: for dust,  $\mu_g = 0.4\text{ }\mu\text{m}$ ,  $\sigma_g = 2.0$  (note that we omit the coarse mode dust distribution by *Phillips et al.* [2008] as the number concentration is very low, a fraction of 1/2000 of the accumulation mode); for soot/black carbon;  $\mu_g = 0.135\text{ }\mu\text{m}$ ,  $\sigma_g = 1.6$ . We note that *Khvorostyanov and Curry* [2004, 2005] assumed that IN mixed with soluble material resided in the nucleation mode, with a typical median radius of  $0.02\text{ }\mu\text{m}$ . However, they only considered a monomodal aerosol distribution and acknowledged that further studies of ice nucleation should include larger sized particles that can serve as IN.

[18] We based our choice of the hygroscopicity parameter of dust,  $\kappa_d$ , on the work of *Koehler* [2007] and *Koehler et al.* [2007]. They measured the CCN and IN activity of dust samples from several different locations around the world, and determined that typical  $\kappa_d$  values ranged between 0.01

and 0.08. We have therefore adopted the value of 0.04 for dust particles. In an internal mixture of these dust particles with a 0.1 volume fraction of ammonium sulfate, the total hygroscopicity parameter,  $\kappa_{d+s}$ , is 0.096. For pure soot, or black carbon, it is reasonable to assume that  $\kappa_{bc} = 0$  [*Dusek et al.*, 2006; *Popovicheva et al.*, 2004], and with a 0.1 volume fraction of soluble material associated with them  $\kappa_{bc+s} = 0.06$ .

[19] The total number concentration is assumed to be  $0.5\text{ cm}^{-3}$  for dust particles and  $1\text{ cm}^{-3}$  for soot particles. The dust concentration assumed in these simulations is based on measured average aerosol concentrations of large particles during INSPECT I [*DeMott et al.*, 2003a] and INSPECT II [*Richardson et al.*, 2007]. The INSPECT studies were conducted at Storm Peak Laboratory in Colorado, USA, which is located at midlatitudes at an altitude of 3210 meters above mean sea level. We therefore assume that these dust concentrations are typical for the free troposphere at these latitudes. The concentrations of particles  $>1\text{ }\mu\text{m}$  measured during INSPECT I and II were in the range of about 0.1 to  $3\text{ cm}^{-3}$  [*DeMott et al.*, 2003a; *Richardson et al.*, 2007]. We note that the PDA08 parameterization is based in part on the IN measurements during INSPECT I and scales predicted IN concentrations based on the measured aerosol loading and surface area during that project, and thus the choice of initial conditions in the parcel model simulations presented here favors the PDA08 parameterization.

[20] Biological particles or organic carbon acting as IN are not included in these studies even though DW04 and PDA08 include them in their parameterizations. Specific knowledge about these types of IN is still limited, and the assumptions of dust and soot in our simulations will in any case point out any significant similarities or differences in the parameterizations compared here.

[21] Figure 1 shows ice crystal and droplet concentrations, ice and water mixing ratios, and saturation ratios as a function of height and temperature in simulations with an initial temperature of  $10^{\circ}\text{C}$  and updraft velocities of (1)  $50\text{ cm s}^{-1}$  and (2)  $500\text{ cm s}^{-1}$ . By starting at  $10^{\circ}\text{C}$ , activation of cloud droplets is completed (i.e., supersaturation with respect to water peaks and begins to decay) before ice crystal nucleation occurs, in all parameterizations. The parcel is lifted to just after the point where homogeneous freezing nucleation starts, which is between 6500 and 7000 m (depending on updraft velocity and parameterization). Note that ice crystal and droplet concentrations are corrected to initial temperature and pressure, i.e., air density effects as the parcel rises and expands are not included in the figures.

[22] The conditions at which the onset of freezing occurs vary greatly between the three different parameterizations. With the KC04 scheme, ice nucleation starts close to  $-11^{\circ}\text{C}$  for the dust case ( $\theta = 50^{\circ}$ ) and close to  $-15^{\circ}\text{C}$  for the soot case ( $\theta = 60^{\circ}$ ). The main differences between the two types of insoluble aerosols acting as IN are the assumed contact angles and the size distributions. While there is a dependence of the freezing rate on size (larger particles may freeze earlier since freezing rate is proportional to the square of insoluble particle radius (see Appendix B, equation (B4)), in these simulations the difference in contact angle is the main reason for the different onset freezing temperature. The nucleation

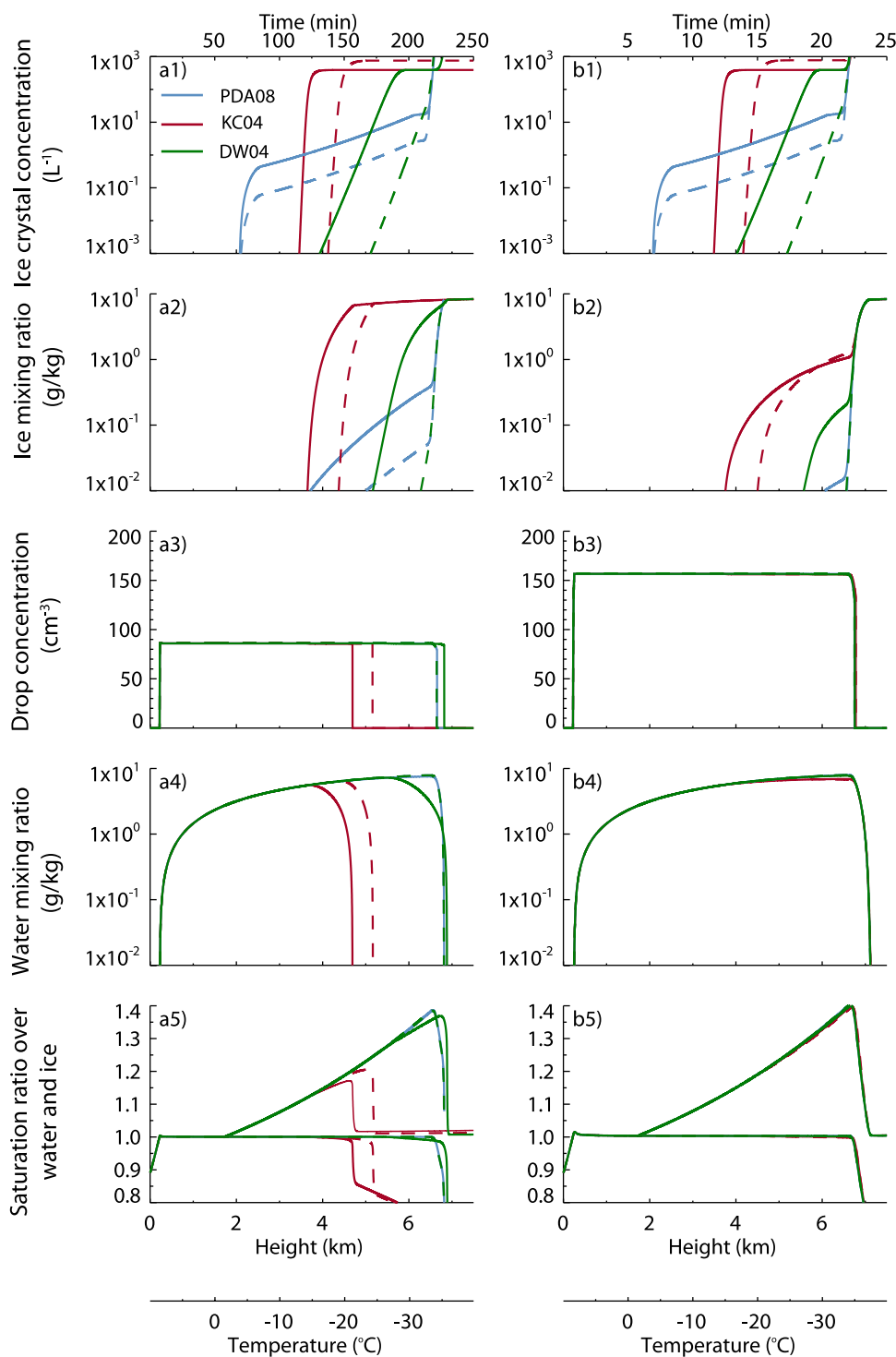


**Figure 1.** Parcel simulations with an initial temperature of 283 K and a pressure of 800 hPa. Blue curves represent PDA08, red curves represent KC04, and green curves represent DW04. Solid curves are for dust as IN and dashed curves are for soot as IN. The Figure 1ax is for an updraft of  $50 \text{ cm s}^{-1}$  and Figure 1bx is for an updraft of  $500 \text{ cm s}^{-1}$ .

rate is large at the onset of freezing and ice crystal concentrations of  $500 \text{ L}^{-1}$  for dust and  $1000 \text{ L}^{-1}$  for soot are quickly reached for both updraft velocities, i.e., all insoluble particles activate ice formation.

[23] In applying KC04, we have assumed that  $\alpha = 0$ , thus the particles do not have any active sites for which the contact

angle is  $0^\circ$ . The elastic strain is also assumed to be zero. These values are the same as those assumed in baseline runs in a few modeling studies using KC04 [Khvorostyanov and Curry, 2005; Khvorostyanov et al., 2006]. By including active sites the onset of freezing would occur earlier because of more efficient freezing. Further, if assuming a misfit strain

of  $\varepsilon = 1\%$ , the freezing temperature would decrease an additional  $2^\circ\text{C}$ , while  $\varepsilon = 2\%$  decreases the freezing temperature by about  $6^\circ\text{C}$  [Turnbull and Vonnegut, 1952].

[24] Compared to parcel model simulations in *Khvorostyanov and Curry* [2005] (hereafter called KC05) the freezing rate here is generally steeper since the particles that contribute to IN are larger and therefore more efficient in freezing. Also, we note that sensitivity studies in KC04 and KC05 only include freezing of haze particles (or residual interstitial diluted particles after drop activation, termed deliquescence heterogeneous freezing). Here we also include immersion freezing (i.e., freezing of activated droplets) in the simulations since activated droplets can contain potential ice nuclei, and there are no reasons for assuming that only nonactivated haze droplets freeze in clouds.

[25] Shortly after the initiation of ice nucleation, droplets start to evaporate in the  $50\text{-cm s}^{-1}$  simulation since ice crystals grow at the expense of water droplets because of the lower vapor pressure over ice than over water (WBF processes). In the KC04 case, the ice crystal concentration is so high that loss of vapor to the growing ice crystals largely overpowers the ice supersaturation generation in the updraft. A complete glaciation effect is therefore seen as all droplets quickly evaporate. The decrease in supersaturation is not evident until the very end of the  $500\text{-cm s}^{-1}$  simulation, since supersaturation generation is strong enough to sustain both ice crystals and droplets. Homogeneous nucleation is initiated near the end of the  $500\text{-cm s}^{-1}$  simulation, because the water saturation ratio is high enough and temperature low enough to support homogeneous freezing. However, the supersaturation quickly decreases after the initiation of homogeneous nucleation.

[26] Using the PDA08 parameterization (blue curves), ice nucleation starts at  $-2^\circ\text{C}$  for both soot and dust. The increase of ice crystals with height is slow for both types of aerosols, as the PDA08 parameterization has a “built in” control of the maximum fraction of a population of insoluble particles that may act as IN at a given temperature and ice supersaturation. The numbers of IN never equal the total number of particles in the larger aerosol mode. Thus more time spent at these temperatures and ice supersaturations would not nucleate more ice crystals, in agreement with the singular hypothesis. As the parcel rises, more ice crystals continue to form, but a level of ice activation and growth for which the WBF process and negative ice saturation feedbacks halts further ice crystal nucleation is not reached. Homogeneous nucleation is predicted at the end of the simulation for all IN and updraft cases. Prior to the onset of homogeneous freezing nucleation, the predicted ice crystal concentrations using the PDA08 scheme are close to two (three) orders of magnitude less than predicted with the KC04 scheme for dust (soot).

[27] The DW04 parameterization allows for freezing to start at  $0^\circ\text{C}$ . However, the initial ice crystal number concentration generated is low and the DW04 parameterization predicts a later freezing onset than the other parameterizations. The change in ice crystal concentration with height is slower than in the KC04 scheme, but for the most part steeper than the PDA08 parameterization. Therefore there is a large difference in ice crystal concentrations at a given height between the different parameterizations. As in the KC04 simulation, the DW04 parameterization also allows

all insoluble particles to freeze if the parcel is lifted high enough.

[28] The simulations with  $50\text{ cm s}^{-1}$  updraft span several hours. In a realistic case, mixing, entrainment, sedimentation and possible radiative effects would change the characteristic of the parcel over this timescale, and the low updraft would probably not be maintained for this long of a period. Thus although the KC04 and DW04 parameterizations predict a final freezing fraction of one (all insoluble particles act as IN) in the simulations shown in Figure 1, limiting the parcel rise to a lower altitude could lead to very different ice crystal concentrations predicted by the two parameterizations. If a temperature profile (or stability) were used as the driving force for uplift (as done for example by *Diehl et al.* [2006, 2007]), the differences in latent heat release between some of the parameterizations could lead to differences in buoyancy and cloud thickness.

[29] In the cold cases (Figure 2) the simulations start at  $-14^\circ\text{C}$  and the updraft velocities assumed are 5 and  $50\text{ cm s}^{-1}$ . The onset of freezing with dust as IN for both the PDA08 and KC04 parameterizations starts at water subsaturated conditions, although close to water saturation. This is due to the deliquescence freezing mechanism in the KC04 framework, and from an enhancement term for ice formation via immersion and condensation freezing included in the PDA08 parameterization. Again, the predicted ice crystal number concentrations are very different between the different parameterizations. This also leads to large differences in the temporal (vertical) profile of cloud droplet concentrations. The KC04 scheme does not allow for any droplets to form at any updraft velocity in the case with dust as IN; the saturation ratio quickly decreases after the onset of ice formation in these cases and the water saturation ratio never reaches unity. Droplets (mixed-phase cloud conditions) are predicted for a short time period in the  $50\text{-cm s}^{-1}$  updraft that assumes the IN are soot. With the PDA08 parameterization, cloud droplets are predicted to form in all cases, but only a few droplets are activated at low updraft velocities in the dust case before they are quickly evaporated because of the WBF process. In the simulations with the DW04 parameterization water supersaturation is reached in all cases and peak water supersaturations are reached. Only after further uplift to about 1.2 km do droplets start evaporating in the low updraft dust case, and even later in the remaining cases.

[30] The predicted final ice crystal concentrations are lower for all parameterizations in the  $5\text{-cm s}^{-1}$  updraft case than in the  $50\text{-cm s}^{-1}$  case. This is due to slower supersaturation generation rates but similar supersaturation depletion rates from droplet and ice crystal growth (in the initial part of the simulation the ice crystal concentrations are the same in both cases), causing supersaturation to peak earlier than at higher updraft velocities. Decreasing supersaturation stops further ice crystal formation. Through this effect, ice crystal nucleation is basically limited, and all parameterizations (except the soot case using PDA08) predict a low fraction of aerosol particles forming ice crystals. The ice crystal concentration predicted from soot IN using PDA08 is small enough that growth of ice crystals does not deplete the vapor. On the basis of the frequent negative feedback of ice nucleation via supersaturation depletion that they observed in their simulations, KC05 suggested that the generally lower concentrations of ice crystals in clouds

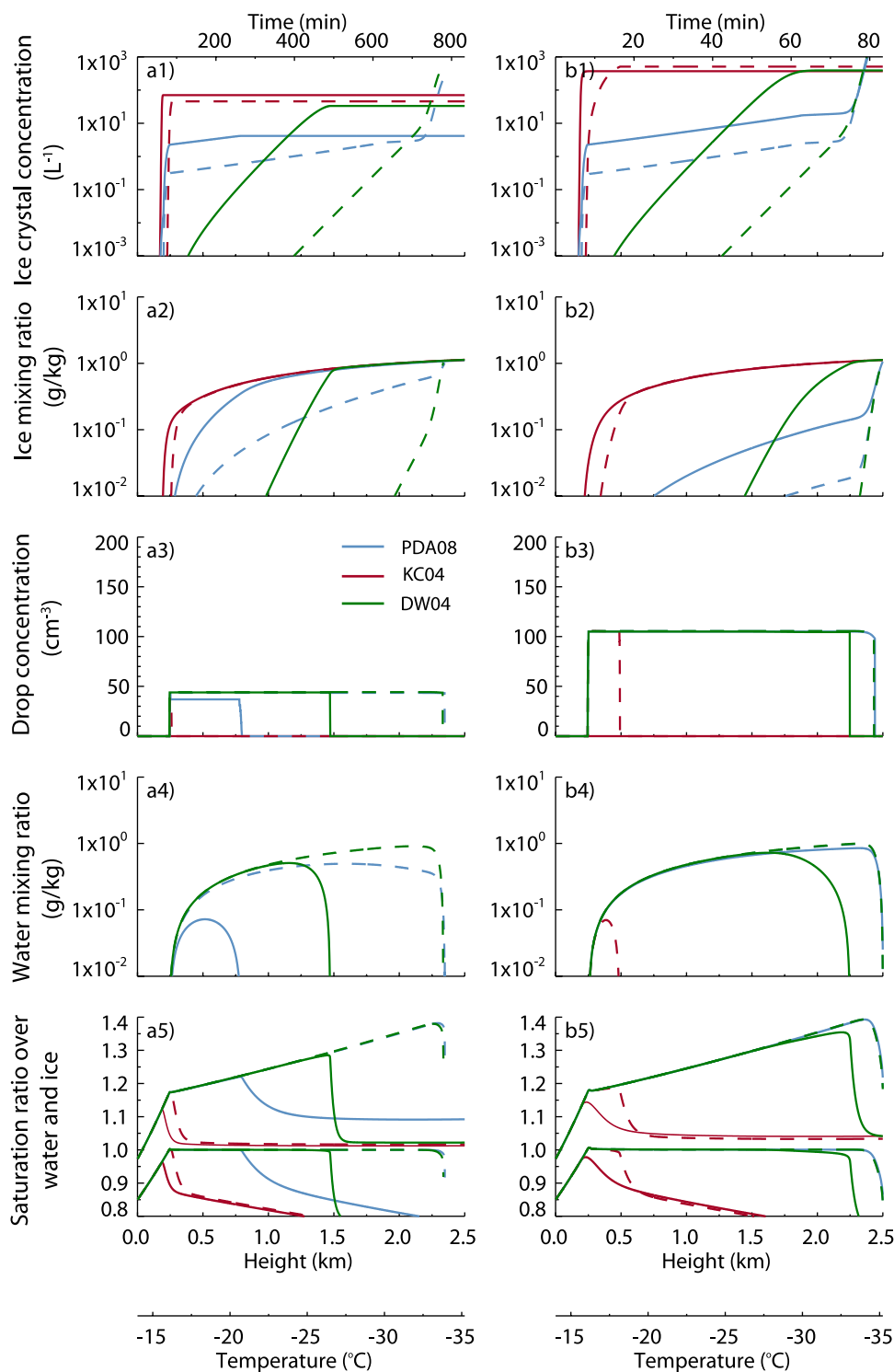


**Figure 2.** Same as Figure 1 but for an initial temperature of 259 K and assumed updraft velocities of (ax)  $5 \text{ cm s}^{-1}$  and (bx)  $50 \text{ cm s}^{-1}$ .

compared to droplets might not be due to much lower number concentrations of IN compared to CCN, but might instead be due to slow ice nucleation combined with fast ice crystal growth, that is, the number concentration of ice is limited by the depletion of supersaturation by rapid growth (a “negative feedback” on ice nucleation at certain updraft speeds). In contrast, droplets activate quickly and grow slowly, such that

depletion of supersaturation in liquid clouds is only rapid enough to compete with supersaturation generation if high number concentrations of activated droplets are generated.

[31] To further investigate the effect of the negative feedback on ice nucleation with the different parameterizations, we conducted a series of simulations with several different updraft velocities ( $0.5$  to  $500 \text{ cm s}^{-1}$ ) and initial dust number

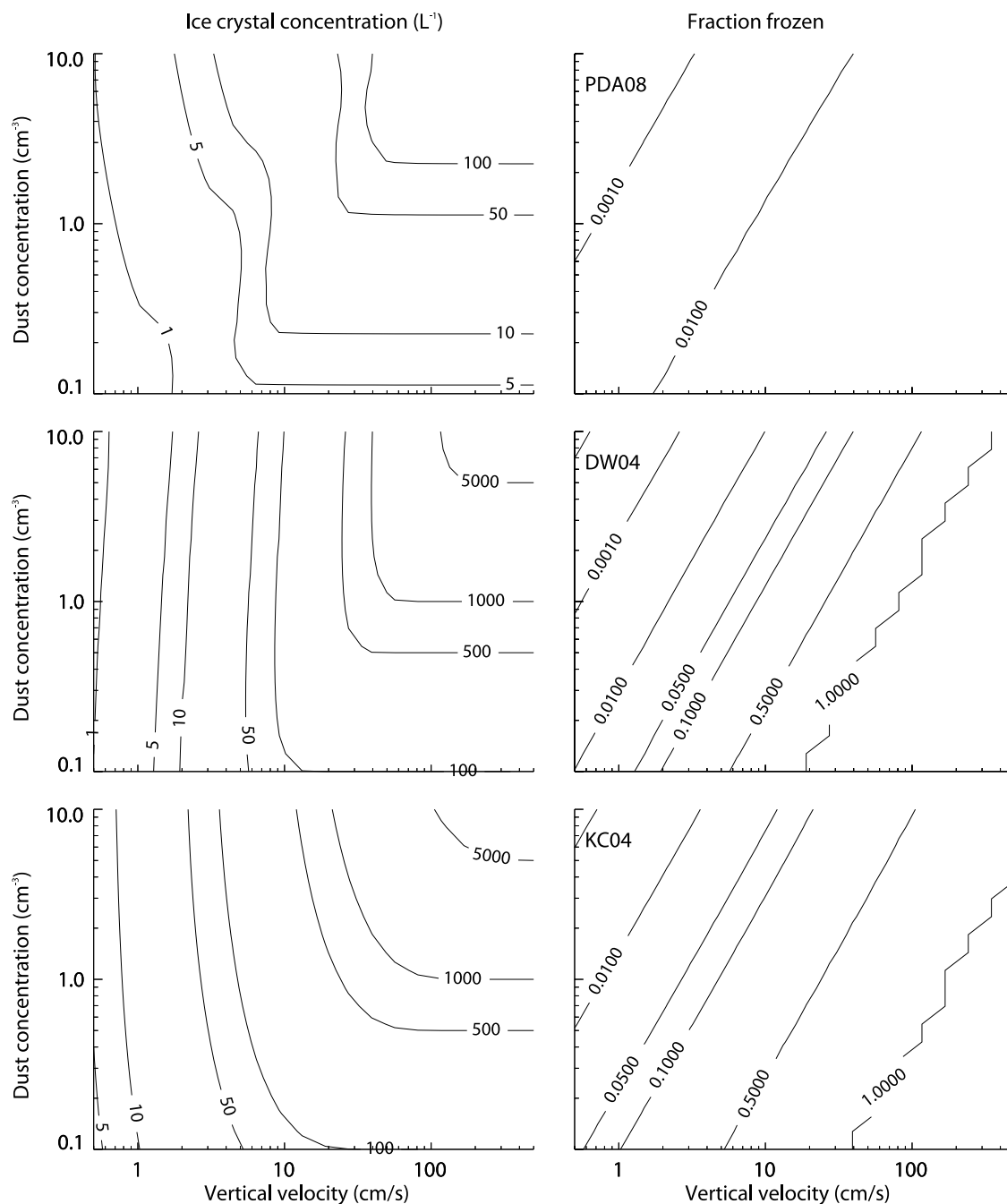


**Figure 3.** (left) Contours ( $\text{L}^{-1}$ ) of predicted ice crystal concentrations as functions of updraft velocity and initial dust concentration. (right) Contours of fraction frozen from the initial dust concentrations. The nonsmooth line for a frozen fraction of 1 is due to the maximum limitation of dust concentration in the simulations.

concentrations ( $0.1$  to  $10 \text{ cm}^{-3}$ ). The initial conditions are the same as for Figure 2 ( $T_{\text{initial}} = -14^\circ\text{C}$  and  $P_{\text{initial}} = 800 \text{ hPa}$ ) and the parcel was lifted to  $3000 \text{ m}$ . Only heterogeneous nucleation was allowed. Figure 3 (left) shows the predicted contours of ice crystal number concentration as functions of updraft velocity and initial dust particle number concentration. The top plots represent the PDA04 parameterization, middle plots the DW04 parameterization and the lower plots represent the KC04 scheme. Figure 3 (right) shows contours of the predicted frozen fraction from the initial dust concentration.

[32] The vertical contour regions in the ice crystal concentration plots indicate where the predicted ice crystal number concentration is independent of the initial number concentration of dust, and only controlled by the updraft. However, the three parameterizations still differ from each other in predicted ice crystal number concentrations in these regions because of different predicted onset of freezing conditions and freezing rates. For example, below updraft velocities of about  $3 \text{ cm s}^{-1}$ , PDA08 and DW04 predict about the same ice crystal concentration, while KC04

predicts almost an order of magnitude higher concentrations. As the updraft velocity increases, the parcel can support higher number concentrations of ice crystals and the final ice crystal concentrations are controlled by the amount of dust, represented by regions of horizontal curves. Note that we have assumed that the ice crystals are spherical in the growth calculations and that the deposition coefficient has a value equal to 1. Different assumptions will move the contours, but the qualitative conclusions will not change.

[33] All these simulations indicate that, in convective systems, we can expect the different parameterizations to predict much different ice crystal number concentrations because of heterogeneous ice nucleation. In Arctic stratiform clouds where effective updraft velocities can be less than  $1 \text{ cm s}^{-1}$ , one could expect the parameterizations to predict similar ice crystal concentrations because of the negative feedback processes. However, the updraft velocities might exceed  $50 \text{ cm s}^{-1}$  because of turbulent motion, and in such cases, the ice crystal concentrations predicted by the different parameterizations can be rather different.

## 5. Susceptibility of Cirrus Cloud Properties to Heterogeneous Nucleation

[34] Cirrus clouds forming in-situ (as distinguished from convective anvil clouds) are typically formed by homogeneous nucleation of haze particles at  $T < 40^\circ\text{C}$  [e.g., *Heymsfield and Miloshevich, 1993; Sassen and Dodd, 1988*]. However, heterogeneous nucleation on insoluble particles can initiate ice formation at warmer temperatures and lower ice supersaturations than required for homogeneous nucleation. The onset of heterogeneous nucleation earlier in a rising parcel might inhibit homogeneous nucleation at colder temperatures because of the depletion of vapor by the growing ice crystals. If this occurs, the number concentration of ice crystals can be suppressed (the “negative Twomey effect” for cirrus clouds [*Kärcher and Lohmann, 2003*]) and the ice crystals can grow to larger sizes, changing the radiative characteristics of the cirrus cloud. In addition, large ice crystals sediment more effectively, thus there are potential effects on cloud lifetime and on the humidity in the upper troposphere and stratosphere [*Jensen et al., 2001*].

[35] Several papers reporting the effects of heterogeneous ice nucleation on cirrus clouds have been published [*DeMott et al., 1997, 1998; Gierens, 2003; Kärcher and Lohmann, 2003; Kärcher et al., 2006, 2007; Khvorostyanov and Curry, 2005; Liu and Penner, 2005*]. *Gierens [2003], Liu and Penner [2005], and Kärcher et al. [2006]* developed parameterizations for the competition between homogeneous and heterogeneous nucleation for use in global- or large-scale models. *Liu and Penner [2005]* developed parameterizations for the critical initial soot concentration in the immersion mode for which heterogeneous nucleation dominates over homogeneous nucleation, and for the transition regime where homogeneous and heterogeneous nucleation occur simultaneously. Heterogeneous nucleation in their model is based on the classical heterogeneous ice nucleation theory. *Gierens [2003]*, on the other hand, developed a parameterization for the critical ice crystal number concentrations nucleated from soot particles following the ice nucleation parameterization of *DeMott et al. [1997]* for freezing by the soot particles.

However, this parameterization does not account for the transition regime. The parameterization developed by *Kärcher et al. [2006]* is based upon a modification of homogeneous freezing theory and simulates the competition between heterogeneous and homogeneous freezing with a parameterized nucleation rate. It allows for varying the freezing efficiency of different particle types by assuming a critical supersaturation for which heterogeneous freezing occurs that is lower than for homogeneous nucleation. The number of ice crystals that can be formed from heterogeneous nucleation must be assumed beforehand. Thus there is no predictive/empirical link between the aerosol number concentration/size distribution and IN concentrations in this parameterization.

[36] Here we present results from simulations of competition between heterogeneous and homogeneous nucleation, similar to previous studies. However, we focus on dust rather than on soot when comparing the three different heterogeneous ice nucleation parameterizations. An in-depth consideration of the state of knowledge of how soot may affect cirrus clouds has been published by *Kärcher et al. [2007]*, and indicates that the role of soot as IN is less understood than is the role of dust. To study the competition between homogeneous and heterogeneous nucleation, 400 simulations were conducted, varying updraft velocity and initial dust number concentrations ( $N_D$ ), as in the simulations for Figure 3.  $N_D$  was varied from  $10^{-4}$  to  $10 \text{ cm}^{-3}$  while the velocities were varied from  $0.5$  to  $50 \text{ cm s}^{-1}$ . The lower velocities characterize synoptic forcing of cirrus while the higher velocities are typical of mesoscale vertical winds during cirrus cloud conditions [e.g., *Haag and Kärcher, 2004*]. The same size distributions as described in section 4 were used here, and homogeneous and heterogeneous nucleation were allowed to proceed simultaneously. We chose the same initial condition for warm cirrus as used by *Lin et al. [2002]* with initial temperature, pressure and relative humidity with respect to ice set to  $-40^\circ\text{C}$ ,  $340 \text{ hPa}$  and  $100\%$  respectively.

[37] Figure 4 (left) shows contours with predicted ice crystal number concentrations using PDA08, DW04, and KC04, for the selected ranges of vertical velocity and initial dust number concentrations. Figure 4 (middle) shows the percent differences in the number of nucleated ice crystals between a simulation where only homogeneous nucleation is allowed ( $N_{i,hom}$ ) and simulations where both heterogeneous and homogeneous nucleation are allowed ( $N_{i,hom+het}$ ). Figure 4 (right) shows the dominant nucleation process for the different updraft velocities and initial  $N_D$ .

[38] For the initial conditions considered here, Figure 4 indicates that a negative Twomey effect is generally seen where heterogeneous nucleation is the dominant control on ice particle number concentrations. There is, however, the transition regime between control by heterogeneous nucleation and control by homogeneous nucleation. In this regime, some ice crystals are formed heterogeneously, but the concentration is not large enough to suppress supersaturation, thus homogeneous nucleation takes place when the parcel reaches the right conditions. This can be seen in Figure 5, which shows ice crystal concentration, ice supersaturation and ice water content as a function of height. Figure 5c, specifically, shows a simulation in the PDA08 transition regime, where updraft velocity is  $24 \text{ cm s}^{-1}$  and

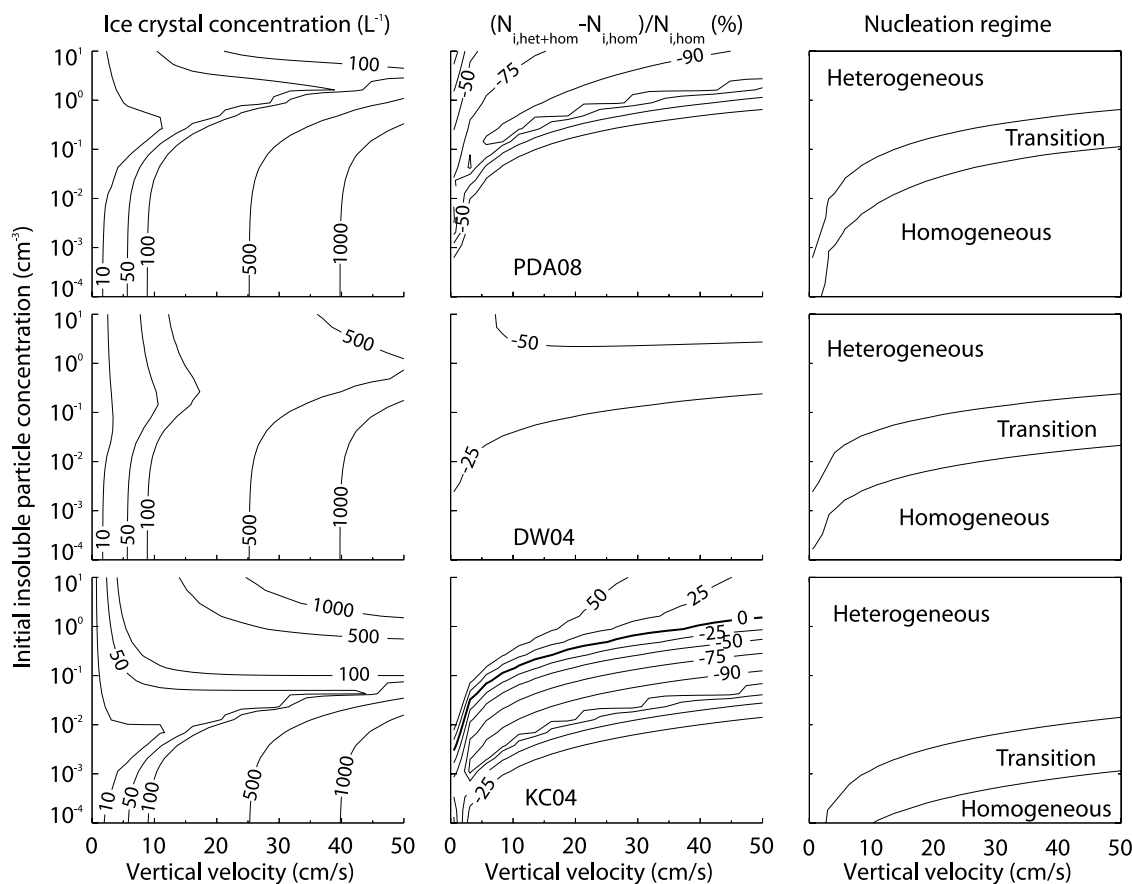


**Figure 4.** Competition between homogeneous and heterogeneous nucleation. (left) Contours of predicted ice crystal concentrations ( $L^{-1}$ ) as a function of updraft and dust concentration. (middle) Contours of the percent difference from simulations with only homogeneous nucleation and simulations where both homogeneous and heterogeneous nucleations are allowed to proceed. (right) Regions where homogeneous or heterogeneous ice nucleation is dominant.

initial dust concentration is  $0.078 \text{ cm}^{-3}$ . The black curve represents the simulation where only homogeneous freezing is allowed, while the blue curve represents the PDA08 simulation. In the PDA08 transition regime, only a few ice crystals are formed heterogeneously early in the simulation before homogeneously produced ice crystals are formed. The total ice crystal number concentration is slightly lower than for the case of homogeneous nucleation alone, and the maximum supersaturation is almost the same in both cases. Figure 5d, on the other hand, shows a case for the PDA08 parameterization where the ice crystals are all formed heterogeneously and maximum supersaturation is about 20% lower than for a pure homogeneous case. Figures 5a and 5b show PDA08 simulations where homogeneous nucleation is not affected by early heterogeneous nucleation.

[39] The PDA08 simulation predicts that heterogeneous nucleation controls the number concentrations of ice crystals for low dust concentrations only at very low updraft velocities. At higher updraft velocities, heterogeneous nucleation is dominant for initial  $N_D$  greater than about  $0.1\text{--}1 \text{ cm}^{-3}$  (depending on updraft velocities). For the simulations with the DW04 parameterization the heterogeneous nucleation dominated regime is extended toward lower initial dust concentrations (see Figure 4). Also, the negative Twomey effect is not as strong as in the PDA08 simulation since the

DW04 parameterization tends to predict higher ice crystal concentrations. As can be seen in Figure 5 (green curves), the heterogeneous formation of ice does not initiate much earlier than does homogeneous nucleation. The reason is that freezing in DW04 is based on measured median freezing temperatures, and early onset freezing is not captured. Thus even if all ice crystals are formed heterogeneously (Figures 5c and 5d), the difference in supersaturation from a pure homogeneous case is not as large as predicted with the PDA08 parameterization.

[40] The simulation with the KC04 scheme shows a distinctly different result for the Twomey effect. Only for very low dust concentrations is homogeneous nucleation dominant (see Figure 5). This simulation also shows a positive Twomey effect for the initial conditions considered. In high dust loadings, more ice crystals can be formed heterogeneously than homogeneously, using this parameterization. As a consequence the supersaturation in most cases considered here is about 20–30% lower than in the cases with only homogeneous nucleation.

[41] We note that heterogeneous ice nucleation from each individual parameterization at all updrafts starts at about the same time (same height and ice saturation ratio). Further, the KC04 and PDA08 parameterizations are also comparable with each other in the starting point of heterogeneous ice

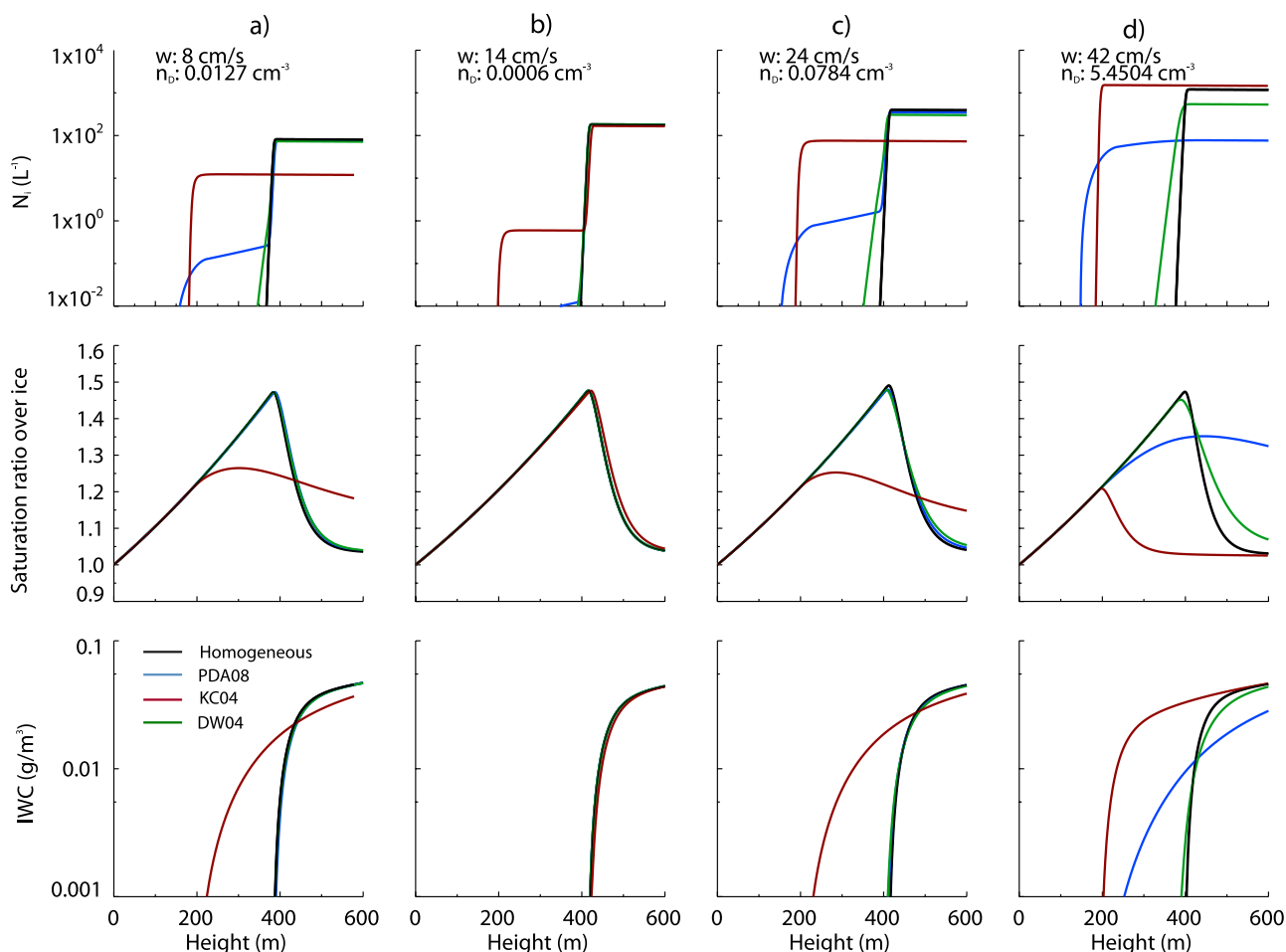


**Figure 5.** Selected simulations from Figure 4 showing ice crystal concentrations, saturation ratio over ice, and ice water content as a function of height. Black curves represents simulations where only homogeneous nucleation is allowed. Red curves represent KC04, blue curves represent PDA08, and green curves represent DW04. The assumed updraft velocities and dust number concentrations are given for each different simulation.

nucleation. However, this is a coincidence for this specific case. The KC04 parameterization takes water activity into account, while PDA08 is only a function of temperature and ice saturation ratio. For example, in the same type of simulations above, but with initial starting temperature of  $-60^\circ\text{C}$ , heterogeneous ice nucleation in PDA08 starts at lower ice saturation ratio than at warmer temperatures, irrespective of solute concentration of the mixed CCN. On the other hand, heterogeneous ice nucleation with the KC04 parameterization starts at higher ice saturation ratio than for the  $-40^\circ\text{C}$  simulations, since solute concentration is higher in the cold case [Lin *et al.*, 2002, Figure 6], and KC04 takes water activity into account (simulations not shown here).

## 6. Critical Discussion of Heterogeneous Ice Nucleation Parameterizations in Relation to Observations of IN

[42] Atmospheric measurements should be the standard against which parameterizations are compared. Here we present a comparison between model simulations and measurements of IN from field campaigns using the Colorado State University Continuous Flow Diffusion Chamber

(CFDC). The primary data chosen for comparison are the measurements from the INSPECT campaigns, since these data were used to constrain the PDA08 parameterization and because the baseline aerosol size distribution used for earlier simulations is based on an average one measured during these programs.

[43] We first address any possible instrumental issues that might impact the IN measurements. It should be recognized that a CFDC measures ice nuclei activation and ice crystal growth over a wide dynamic range without the influence of water vapor competition. This was a key aspect of the continuous flow instrument design as described by Rogers [1998]. Thus the instrument has been shown to observe nucleation of up to  $100 \text{ cm}^{-3}$  ice crystals within the homogeneous freezing nucleation regime [DeMott *et al.*, 2003a]. These are much higher number concentrations than would be expected or have ever been measured from heterogeneous nucleation, so it is reasonable to assume that the CFDC is capable of detecting the maximum number concentration of IN available for activation (in the condensation, immersion, deposition and deliquescence mode) in the atmosphere for the same ambient temperature and relative humidity as the processing temperature and humidity. Full validation of this

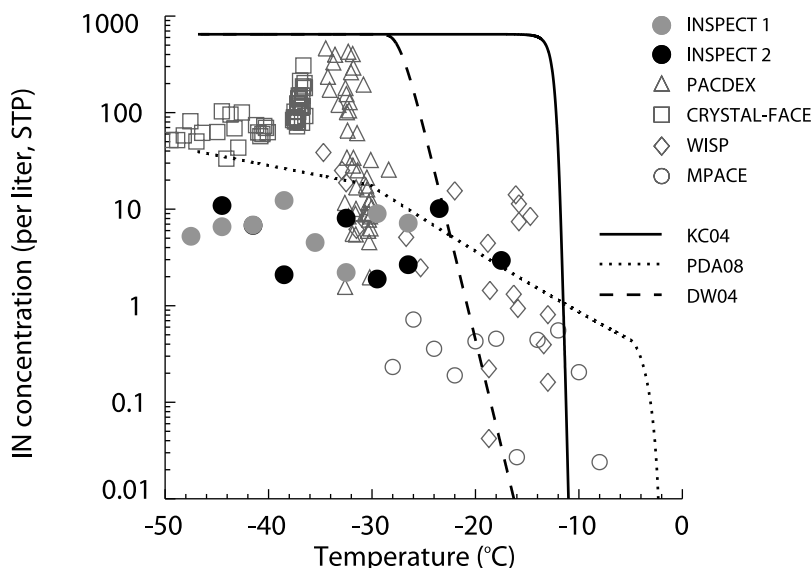


**Figure 6.** Ice nuclei number concentration (at standard temperature and pressure) measured with the CFDC from several different field campaigns in the free troposphere. Filled symbols represent measurements from INSPECT I (grey [DeMott *et al.*, 2003a]) and INSPECT II (black [Richardson *et al.*, 2007]) binned into 3°C temperature intervals, on which we base the initial insoluble aerosol concentrations in the parcel model simulations. Selected 1-min average concentrations from 3 days during PACDEX [Stith *et al.*, 2009] are from over the north Pacific, in and out of intense Asian dust layers. CRYSTAL-FACE (Cirrus Regional Study of Tropical Anvils and Cirrus Layers-Florida Area Cirrus Experiment) measurements are from directly within the Saharan Aerosol Layer near Florida [DeMott *et al.*, 2003b; Prenni *et al.*, 2007a]. WISP (Winter Icing in Storms Project) data from the winter–spring transition period in Colorado are adapted from the study of Möhler *et al.* [2007]. MPACE measurements are obtained in Arctic Fall [Prenni *et al.*, 2007b]. Curves represent ice crystal concentrations predicted in the parcel model with an updraft of  $500 \text{ cm s}^{-1}$  and the background aerosol size distribution. The solid curve shows predictions with the KC04 scheme, dashed curve with the DW04 parameterization, and dotted curve with the PDA08 parameterization.

assumption must await proof that time dependence is not a strong factor in nucleation by the noted ice formation mechanisms, and publication of results from recent “closure” studies in which IN number concentrations were compared directly to ice crystal concentrations in clouds [DeMott *et al.*, 2008].

[44] The CFDC has an upper aerosol size limit of about  $1.5 \mu\text{m}$  for detecting IN. Since the concentration of such large particles is typically very low and only a small fraction of even 1 micron dust particles are active as IN in the mixed-phase cloud regime [Field *et al.*, 2006], the undercounting of IN due to ignoring supermicron particles is expected to be low. Nevertheless, this remains as an uncertainty in circumstances with elevated supermicron loadings.

[45] Real-time IN measurements such as the CFDC also allow less than 10 s for ice nucleation to proceed. Nevertheless, new evidence for the deterministic nature of mechanisms besides contact freezing support the validity of “fast” IN measurement methods [DeMott *et al.*, 2008]. In these studies, IN concentrations measured by the CFDC and other continuous flow IN instruments predicted within a factor of  $\sim 3$  the number concentrations of mineral dust and bacterial IN activating in few minute duration expansion cloud formation experiments in the AIDA (Aerosol Interactions and Dynamics in the Atmosphere) cloud chamber [e.g., Möhler *et al.*, 2006].

[46] The comparisons of ice nuclei number concentrations versus predicted ice crystal number concentrations of heterogeneous ice nucleation need to be made for the maximum ice crystal concentrations possible for a given set of thermodynamic conditions, thus the simulations should not allow for insufficient vapor (or negative feedback) to be a factor. Figure 6 shows IN number concentration as a function of temperature measured with the CFDC from the INSPECT campaigns (solid circles). Also shown are measured IN concentrations from several other field campaigns (see caption). There are large variations of IN concentrations between the different field campaigns, corresponding to large variations of aerosol concentrations (not shown here). For example, the CRYSTAL-FACE and some of the PACDEX measurements were obtained from within airborne Saharan and Asian mineral dust plumes with mass concentrations up to  $80 \mu\text{g m}^{-3}$ . Differences in processing water relative humidity ( $\text{RH}_w$ ) are also reflected to some degree. Nevertheless, most of the measurements at temperatures warmer than  $-35^\circ\text{C}$  have been obtained for  $\text{RH}_w$  values in excess of 100% and so can be viewed as the highest expected number concentration of IN available at these temperatures. Also shown in Figure 6 are the predicted ice crystal concentrations for the dust cases from the simulation in Figure 1 at  $500 \text{ cm s}^{-1}$ . In this particular simulation, there were no negative vapor feedbacks for any of the runs using the three parameterizations. The initial dust concentration ( $0.95 \mu\text{g m}^{-3}$  mass

concentration for diameter  $<2.5 \mu\text{m}$ ) for parcel simulations in Figure 1 (and Figure 2) is based on the INSPECT measurements. Therefore we should expect the simulations to compare best with the INSPECT measurements.

[47] The PDA08 parameterization is expected to compare best with the INSPECT measurements, since those measurements were used in the development of the parameterization and since measured surface areas are used as inputs to the parameterization. The PDA08 parameterization predicts ice crystal concentrations closest to, though slightly higher than measurements (by a factor of 2 or 3). The main reason for the difference arises from the input dust loading. PDA08 based the “reference” or baseline dust mode concentration in their parameterization on aerosol mass and surface area concentration data collected in the INSPECT I campaign. However, the measured IN number concentrations from INSPECT I are lower by less than a factor of 2 for equivalent sampling conditions compared to INSPECT II, while the aerosol loading during INSPECT I is lower by a factor of at least 7 compared to INSPECT II. We have used as input to the model runs the average dust concentration from both INSPECT I and INSPECT II. The KC04 and DW04 parameterizations overestimate ice crystal concentrations by orders of magnitude compared to the IN measurements. The measurements that show IN concentrations closer to those predicted by DW04 and KC04 (i.e., IN concentrations over  $100 \text{ L}^{-1}$ ) are from the CRYSTAL-FACE (squares) and PACDEX (triangles) field campaigns. However, in both of these campaigns, the measurements were obtained in air masses with high dust mass and particle number loading, originating from the Saharan desert (CRYSTAL-FACE [DeMott *et al.*, 2003b; Sassen *et al.*, 2003] and from major dust sources (Taklamakan and Gobi deserts) in Asia (PACDEX) [Stith *et al.*, 2009].

[48] As a simple test of the robustness of the conclusions made on the basis of the INSPECT measurements that favor the PDA08 parameterization, we performed simulations (not shown) using aerosol size distribution data from the PACDEX dust layer vertical profile presented in Figure 2 of Stith *et al.* [2009]. In these measurements, number concentrations of particles larger than  $0.5 \mu\text{m}$  peaked at about  $5 \text{ cm}^{-3}$  and CFDC IN measurements at  $-32^\circ\text{C}$  reached  $40 \text{ L}^{-1}$ . In this case, the PDA08 parameterization predicted ice crystal concentration of  $100 \text{ L}^{-1}$ , while the DW04 and KC04 parameterizations predicted  $9 \text{ cm}^{-3}$  (the entire dust particle population) activating ice formation.

[49] Since DW04 and KC04 do not have direct constraints on the maximum predicted ice crystal concentration in relation to the insoluble particle concentration, the use of these parameterizations can potentially lead to large over-prediction of ice crystal concentrations. Although these parameterizations may predict realistic ice crystal concentrations in some cases, this is likely driven by negative feedbacks and not by accurate prediction of ice nucleation. Thus assertions made using these parameterizations that high concentrations of ice forming in some cloud conditions may explain previously unresolved ice formation mechanisms must be regarded as a likely artifact of the parameterizations. For example Khvorostyanov and Curry [2005] argued that they could quantitatively predict, using the deliquescence freezing theory of mixed CCN, the rapid ice crystal nucleation in warm maritime polar clouds

( $-5$  to  $-10^\circ\text{C}$ ) as observed by Hobbs and Rangno [1990] and Rangno and Hobbs [1991]. The rapid increase of ice crystal concentrations from less than  $1 \text{ L}^{-1}$  to  $300\text{--}1100 \text{ L}^{-1}$  at  $-5$  to  $-10^\circ\text{C}$  has not otherwise been explained to this point by known ice formation processes, including secondary ice formation by the Hallett-Mossop riming splintering processes. However, we note here that measurements do not indicate that such high IN concentration exists very often in the atmosphere and never at the temperatures where the rapid increase in ice crystal concentration occurred. Therefore we must question arguments that observations by Hobbs and Rangno [1990] and Rangno and Hobbs [1991] can be explained by deliquescence freezing of mixed CCN, or any other presently known or quantified heterogeneous freezing mechanisms.

[50] The DW04 parameterization has been used in several global-scale modeling sensitivity studies [e.g., Lohmann and Diehl, 2006; Lohmann *et al.*, 2007; Storelvmo *et al.*, 2008]. These sensitivity studies have partly focused on the importance of dust IN on modifying the anthropogenic indirect effects of assumed black carbon ice nuclei. In the application of the DW04 parameterization, all dust particles in the accumulation mode can potentially serve as IN in the immersion freezing mode. However, as shown in simulations above, if there are no constraints on the maximum predicted ice crystal concentration in relation to the insoluble particle concentration, the DW04 parameterization can overpredict ice crystal concentrations by several orders of magnitude, especially at temperatures warmer than  $-35^\circ\text{C}$ . Absent realistic quantitative links between insoluble particle number concentrations and ice crystal number concentrations, confidence in accurately simulating the indirect forcing of different classes of IN in present studies must be regarded as very low, even for sensitivity studies. Further, since updraft velocities play an important part in controlling ice crystal concentration, it is important that subgrid vertical velocities are also well characterized in aerosol – ice – cloud studies.

## 7. Constraining Parameterizations

[51] Existing and new data relating ice nuclei to aerosol properties could provide the necessary constraints to correct the noted weaknesses of the KC04 and DW04 parameterizations. For the KC04 simulations we have assumed that all IN have similar surface properties, i.e., that the contact angle, active sites and misfit strain are the same for all dust or soot particles. However, a more realistic representation of heterogeneous freezing would be to introduce a variability of freezing efficiency within each type of particle (singularity assumption). For example, Marcolli *et al.* [2007] showed that heterogeneous freezing measurements of emulsified aqueous suspensions of dust are reproduced correctly in a classical ice nucleation model only when all dust particles are assumed to have different surface properties. By assuming a lognormal distribution of contact angles (geometric mean contact angle of  $76^\circ$  and geometric standard deviation of 1.083) Marcolli *et al.* [2007] could reproduce their measurements reasonably well. Nevertheless, they achieved even better agreement when it was assumed that each particle can have an active site area distribution as a function of contact angle. Thus the different dust particles can be active at different temperatures, and each individual particle can have a range of surface

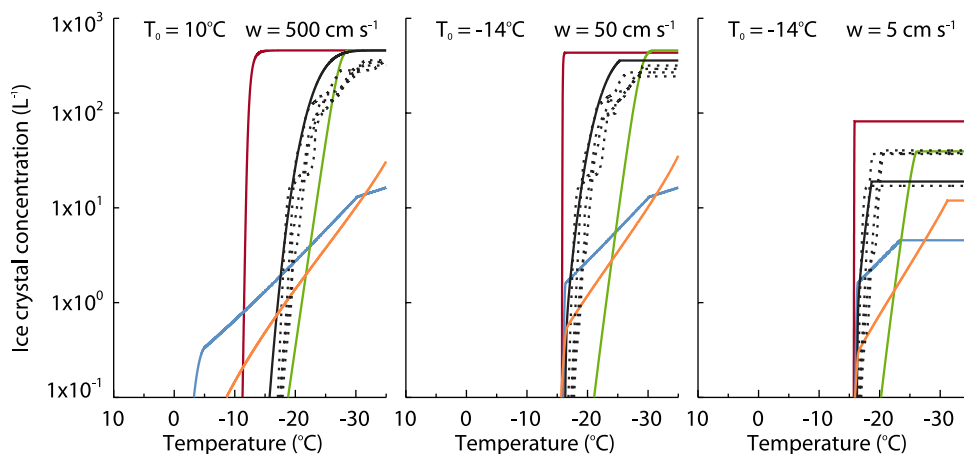


**Figure 7.** Predicted ice crystal concentrations for the 500-cm s<sup>-1</sup> case in Figure 1 and both updraft velocities in Figure 2 (blue curves are with PDA08, red curves with KC04, and green curves with DW04). Included here are simulations using approaches described by Marcolli *et al.* [2007] implemented in the KC04 scheme. Simulations assuming lognormal contact angle distributions are represented with solid black curves and those using active site distributions are represented with dashed black curves. The orange curves show simulations assuming a broad normal contact angle distribution given by equation (1).

properties. Note that the active sites in the study of Marcolli *et al.* [2007] are assumed to be areas with different values of contact angle, while Fletcher [1969] defined the active site to be an area with  $\theta = 0^\circ$ .

[52] We conducted simulations with the KC04 scheme, using both contact angle distribution and active site approaches described by Marcolli *et al.* [2007]. For the active site distribution approach, Marcolli *et al.* [2007] included some randomness of ice nucleation for each individual particle, depending on the critical embryo size (here calculated with equation (B6) in Appendix B) and the active site distribution (see the work of Marcolli *et al.* [2007] for details). We assume here that each particle in each size bin is equal in properties, but the randomness is different between sizes.

[53] Figure 7 shows the predicted ice crystal number concentrations for the same simulations as in Figures 1 and 2 (excluding the 10°C, 50-cm s<sup>-1</sup> simulation). The solid black curve shows the simulation with KC04 assuming the lognormal contact angle distribution. The onset of freezing for the 10°C simulation occurs later than when using a constant contact angle of 50°. This is expected since the geometric mean contact angle from Marcolli *et al.* [2007] is 76° and the standard deviation is rather narrow (without the distribution, freezing would start close to -22°C for a contact angle of 76°). The rate of change in ice crystal concentration with temperature is also less than when assuming a constant contact angle, which comes from the assumption of a distribution of contact angles. However, in the high updraft case, the contact angle distribution approach still allows for almost all particles in the dust mode of the aerosol distribution to act as IN. In the lower updraft cases, the predicted ice crystal concentrations are lower than in the case of constant contact angle because of the negative feedback effect and a slower freezing rate. The dotted black curves show simulations using the active site distribution. Because of the randomness of this approach, we show four simulations. Predicted ice crystal

concentrations are lower than when assuming a lognormal contact angle distribution for all cases in the 500- and 50-cm s<sup>-1</sup> simulations, while there is some more variation in the lowest updraft case. However, overall the predicted crystal number concentrations are still much higher than for the PDA08 parameterization.

[54] To reduce the nucleated ice crystal concentrations further to attempt to align them with the INSPECT measurements, we follow the idea of contact angle distributions but use a different probability function. This approach is taken to see what contact angle distribution can be assumed to better describe measurements using classical nucleation theory. We assume that each individual particle has only one single contact angle over the entire particle, but each size bin is characterized with a distribution of particles with different contact angles. This normalized probability function  $P$  for the contact angles is assumed to be

$$P(\theta) = 2 \cdot N(\mu, \sigma), \quad (1)$$

where  $N$  is the normal distribution, the median  $\mu = 180^\circ$ , standard deviation  $\sigma = 37$  and  $0^\circ < \theta < 180^\circ$ . Note that this probability function was constructed to attempt to match the INSPECT IN measurements. The solid orange curve in Figure 7 shows the predicted ice crystal concentration using equation (1). The use of this probability function in the KC04 scheme clearly reduces the nucleation rate. However, this exercise only demonstrates what possible contact angle distributions might be assumed for classical nucleation theory to compare with IN measurements. Specific measurements must be conducted to determine a more realistic probability function for the contact angle for dust. Note that we have not taken account of active sites for which the contact angle is 0°, or the misfit strain, which are surface parameters in the KC04 scheme that can be varied. An inherent difficulty with using the classical theory for heterogeneous nucleation or variations of it is the strong dependence on such surface property parameters that are not known *a priori* [Pruppacher and Klett, 1997].

[55] The DW04 parameterization also produces large differences between predicted ice crystal concentrations and measured IN concentrations. Assuming that all individual dust or soot particles have the same value for the constant that represents the efficiency of ice nucleation in the immersion mode is probably not realistic. The DW04 scheme could potentially be improved by applying a distribution of freezing efficiencies to better reflect laboratory data on the temperature dependence of the freezing fractions of real dust particle size distributions [Field *et al.*, 2006], as well as applying further empirical constraints obtained from field data.

## 8. Summary and Conclusions

[56] A warm cloud parcel model was modified to include a new parameterization for the treatment of hygroscopicity [Petters and Kreidenweis, 2007], and to include ice nucleation and crystal growth in addition to nucleation and growth of liquid droplets. Homogeneous nucleation was simulated using the parameterization by Koop *et al.* [2000]. Three different heterogeneous ice nucleation parameterizations, which take aerosol composition and number concentration into account, were implemented into the parcel model. Predictions from these parameterizations were compared for parcels rising adiabatically with a constant updraft velocity, over a range of different initial conditions for temperature, updraft velocity, and insoluble aerosol number concentrations. The simulations revealed differences of several order of magnitudes in predicted ice crystal concentration between the parameterizations. This was true when assuming either dust or soot as IN. The PDA08 parameterization predicted the lowest ice crystal concentrations, while KC04 and DW04 were comparable in final concentrations. However, the DW04 parameterization predicts a slower freezing rate than the KC04, which can have a large impact on the predicted phase state (liquid, mixed or ice) of clouds in cases where the height of the air parcel rise is lower than assumed here. Further, the various freezing rates produce different latent heat release rates, modifying parcel buoyancy. Therefore when these parameterizations are used in cloud resolving models, the cloud thickness, amount of precipitation predicted and cloud lifetime in these models can be rather different. Other factors we have not simulated, including ice crystal riming, aggregation, and sedimentation, as well as mixing processes, will complicate IN-cloud interactions, but we still expect the IN parameterizations to have potential to strongly modify cloud model results.

[57] The ice crystal number concentrations predicted for modest to high updraft velocities depend on temperature, on peak supersaturations, and on the number concentration of available IN (Figure 3). For weak updraft velocities, the ice crystal concentrations are controlled by a negative feedback process [Khvorostyanov and Curry, 2005] where rapid growth of ice crystals depletes water and ice supersaturation and halts ice nucleation. Thus lower ice crystal concentrations are predicted at low updraft velocities than for updraft velocities that support high ice supersaturations. The KC04 and DW04 parameterizations could potentially predict ice concentrations in reasonable comparison to PDA08 and to ice concentrations measured in clouds under low updraft velocity conditions.

[58] Predicted ice crystal concentrations in reasonable agreement with the INSPECT IN measurements could be achieved with the KC04 scheme when assuming a normal distribution of dust contact angles but with a rather large standard deviation. This distribution was not based on measurements, but was adjusted to align the predicted ice crystal concentrations with the IN measurements. However, in situ [DeMott *et al.*, 2003a] and laboratory measurements [Koehler *et al.*, 2007] indicate that not all dust or soot particles initiate freezing. Thus not all particles will have active sites with contact angles that can initiate freezing at atmospheric temperatures and supersaturations, and it is reasonable to assume that particles should have a contact angle distribution. It is uncertain what this distribution might be in reality.

[59] We argue that parameterizations must also predict reasonable ice crystal concentrations over a range of updraft velocities, as well as for cases where there are no vapor limitations (or negative feedbacks), in order to be of robust predictive use in models. We therefore conducted a comparison between a parcel model simulation with high updraft velocity (representative of no negative feedback) and IN measurements. The IN measurements were obtained with a CFDC, which operates at a constant ice supersaturation and thus has no vapor limitations in its ability to detect IN. Results from the comparison show that the PDA08 parameterization predicts ice crystal number concentrations closest to measurements. The DW04 and KC04 parameterizations, which are not constrained by field measurements and in this case are not limited by vapor depletion, overpredict ice crystal number concentrations by orders of magnitude compared to the measurements. While this test case compared the predictions from the PDA08 parameterization against data that were used to derive it, we demonstrate that similar conclusions are expected in a more perturbed (dust layer) aerosol scenario. Additional data sets are needed to fully test parameterizations for conditions that they were not explicitly designed for. Nevertheless, our main point is unalterable: a prerequisite for a robust parameterization is that it must limit the maximum predicted drop or crystal number concentrations by the maximum available number concentrations of nucleating particles. Ice nuclei measurements already exist for use in improving model parameterizations and the number and quality of these measurements worldwide will likely be increasing.

## Appendix A: Coupled Differential Equations for Adiabatic Air Parcel Modeling

### A1. Governing Differential Equations

[60] Here we describe the set of governing differential equations in the adiabatic parcel model. We mainly follow Pruppacher and Klett [1997] for a closed parcel (no entrainment). To solve the main set of coupled ordinary differential equations as the parcel is lifted adiabatically we use the Variable-coefficient Ordinary Differential Equation (VODE) procedure by Brown *et al.* [1989]. VODE solves for, as a function of time, the change in the environmental temperature,  $T$ , pressure,  $P$ , and liquid and ice water content through the liquid diffusional and ice depositional growth equations, respectively.

[61] The diffusional droplet growth for droplets, in each size bin  $k$ , is calculated following equations (13.28) of Pruppacher and Klett [1997]:

$$\frac{dD_k}{dt} \approx \frac{4}{D_k} \frac{S_{w,v} - S(D_k)}{\frac{\rho_w TR^*}{D_v^*(D_k) M_w e_{sat,w}(T)} + \left( \frac{L_e \rho_w}{T k_a^*(D_k)} \left( \frac{L_e M_w}{TR^*} - 1 \right) \right)}. \quad (\text{A1})$$

Here  $D$  is the diameter of the droplets,  $S_{w,v}$  the environmental saturation ratio,  $S(D_k)$  the saturation ratio over an aqueous solution drop, and  $\rho_w$  the density of water. The universal gas constant is represented by  $R^*$ ,  $M_w$  is the molecular weight of water, and  $D_v^*$  and  $k_a^*$  are the modified diffusivity and thermal conductivity, respectively (equations (13.14) and (13.20) of Pruppacher and Klett [1997]). Finally,  $L_e$  is the latent heat of evaporation. The revised treatment of water activity of solution drop follows Petters and Kreidenweis [2007], who suggested that particle hygroscopicity can be described using a single parameter  $\kappa$ , and that water activity,  $a_w$ , can be calculated from:

$$a_w^{-1} = 1 + \kappa \frac{V_s}{V_w}, \quad (\text{A2})$$

where  $V_s$  is the volume of the dry particle and  $V_w$  is the associated volume of water. Insoluble, nonhygroscopic particles are represented by  $\kappa = 0$ , and ammonium sulfate aqueous solutions can be represented by  $\kappa = 0.6$  (see the work of Petters and Kreidenweis [2007] for additional tabulated values). The  $\kappa$  of complex internally mixed particles is computed from the sum of the volume-weighted individual component hygroscopicity parameters, assuming that the Zdanovskii, Stokes and Robinson relationship [Stokes and Robinson, 1966] applies. Thus the use of  $\kappa$  allows for straightforward implementation in the model of internally or externally mixed, aerosols. Thus the saturation ratio of a solution drop is expressed as:

$$S(D_k) = a_w \exp\left(\frac{2M_w \sigma_{s/a}}{R^* T \rho_w D_k}\right) = \frac{D_k^3 - D_{k,dry}^3}{D_k^3 - D_{k,dry}^3 (1 - \kappa)} \exp\left(\frac{4M_w \sigma_{s/a}}{R^* T \rho_w D_k}\right), \quad (\text{A3})$$

where  $\sigma_{s/a}$  is the surface tension between the solution droplet and air and  $D_{dry}$  is the dry diameter of the aerosol particle. The term before the exponential represents the water activity, while the exponential represents the curvature (“Kelvin”) effect on vapor pressure over a solution drop. In our simulations we assume  $\kappa$  values that are based on measurements or computations at temperature  $T = 298.15$  K and  $\sigma_{s/a} = 0.072$  J m<sup>-2</sup>. Therefore all calculations involving equation (A3) in the parcel framework are used with these values of temperature and surface tension.

[62] For depositional growth for ice crystals in each size bin  $j$ , we follow equations (13.76) of Pruppacher and Klett [1997]:

$$\frac{dm_j}{dt} \approx \frac{4\pi \rho_i C_j (S_{i,v} - 1)}{\frac{T_\infty R^*}{D_v^*(D_j) M_w e_{sat,i}(T_\infty)} + \left( \frac{L_s}{T_\infty k_a^*(D_j)} \left( \frac{L_s M_w}{T_\infty R^*} - 1 \right) \right)}, \quad (\text{A4})$$

where  $m$  is the mass of the ice crystals,  $S_{i,v}$  is the saturation ratio over ice,  $L_s$  is the specific latent heat of sublimation,  $\rho_i$  the density of ice and  $C_j$  is the capacitance of the crystals. In the parcel model we assume that the crystals are spherical, thus  $C_j = D_j/2$  and the change in ice crystal diameter is

$$\frac{dD_j}{dt} = \frac{2}{\pi \rho_i D_j^2} \frac{dm_j}{dt}. \quad (\text{A5})$$

[63] The total change in liquid or ice water content (here both are described by WC) in the parcel is given by summing the water mass change over all liquid ( $k$ ) and ice ( $j$ ) size bins:

$$\frac{dWC}{dt} = \frac{d}{dt} \sum_{j/k} m_w n(m_w) = \sum_{j/k} \left[ n(m_w) \frac{dm_w}{dt} + m_w \frac{dn(m_w)}{dt} \right], \quad (\text{A6})$$

where  $m_w$  is the water mass  $n(m_w)$  is the number concentration of liquid or ice particles in cm<sup>-3</sup> having water mass  $m_w$ . The first term in the bracket in equation (A6) is given as

$$n(m_w) \frac{dm_w}{dt} = n(m_w) \pi \rho_{w/i} \frac{D^2}{2} \frac{dD}{dt}, \quad (\text{A7})$$

where  $dD/dt$  is given by equations (A1) or (A4). The density  $\rho_{w,i}$  is the water ( $w$ ) or ice ( $i$ ) density. In the parcel framework, the number of particles per gram of air is constant, while the volume of the parcel changes. Therefore the second term in equation (A6) must take changes in air density into account, and is calculated as

$$m_w \frac{dn(m_w)}{dt} = n^*(m_w) \frac{d\rho_a}{dt} \frac{1}{6} \pi \rho_{w/i} (D^3 - D_{dry}^3). \quad (\text{A8})$$

Here  $n^*(m_w)$  is the particle concentration per gram of air and  $\rho_a$  is the air density at the ambient temperature and pressure. The dry diameter of the aerosol particle,  $D_{dry}$ , is subtracted from the cloud particle diameter to only account for the water mass. The air density differential in equation (A8) is dependent on changes in temperature and pressure and is given as

$$\frac{d\rho_a}{dt} = \frac{1}{R_d T^2} \left( T \frac{dP}{dt} - P \frac{dT}{dt} \right), \quad (\text{A9})$$

where  $R_d$  is the gas constant for dry air.

[64] To calculate the environmental changes it is assumed that the environment is in static equilibrium and the pressure differential equation is given as

$$\frac{dP}{dt} = -\rho_a g w, \quad (\text{A10})$$

where  $g$  is the gravitational acceleration and  $w$  is the updraft velocity. The environmental temperature differential equation is expressed as

$$-\frac{dT}{dt} = \frac{1}{c_p} \left( L_e \left( \frac{dw_{v,d}}{dt} + \frac{dw_{v,i}}{dt} \right) + g w \right). \quad (\text{A11})$$

Here  $c_p$  is the specific heat of water at constant pressure. The terms  $dw_{v,d}/dt$  and  $dw_{v,i}/dt$  are the rates of change in

vapor mixing ratio due to liquid droplet growth (subscript  $d$ ) and ice growth (subscript  $i$ ) respectively. These terms are proportional to the change in liquid and ice water content, given in equation (A6). Since the vapor mixing ratio is calculated with the unit of  $g_{\text{water}}/g_{\text{air}}$ , while WC is given as  $g_{\text{water}}/\text{cm}^3_{\text{air}}$ , the change of air pressure must be accounted for when calculating  $dw_v/dt$  (the equation is valid for changes in both liquid and ice droplet content and we have omitted the subscript of ice and droplets here):

$$\frac{dw_v}{dt} = -\frac{d}{dt} \left( \frac{\text{WC}}{\rho_a} \right) = \frac{1}{\rho_a} \frac{d\text{WC}}{dt} - \frac{\text{WC}}{\rho_a^2} \frac{d\rho_a}{dt}. \quad (\text{A12})$$

[65] A change in this parcel model version, compared to earlier versions, is the elimination of the saturation ratio differential equation ( $dS_{w,v}/dt$ ). As long as the parcel is a closed system where entrainment or precipitation is not included, the total water mixing ratio is constant in the parcel. Therefore the differential equation set is overdetermined if  $dS_{w,v}/dt$  is calculated within VODE. While the differential equation solver was able to find adequate solutions for the overdetermined system for liquid clouds, we found that the low vapor pressures over ice in cold clouds led to solutions for which the total water mass was not constant to within the desired accuracy. In this version the saturation ratio is calculated in each internal VODE time step as

$$S_{w,v} = \frac{e}{e_{\text{sat},w}(T)}, \quad (\text{A13})$$

where  $e_{\text{sat},w}(T)$  is the saturation vapor pressure over water and  $e$  is the vapor pressure, calculated from

$$e = \frac{w_v P}{\frac{R_d}{R_v} + w_v}. \quad (\text{A14})$$

Here  $R_v$  is the gas constant for water vapor and  $w_v$  is the vapor mixing ratio calculated as

$$w_v = w_{v,0} - \frac{\text{LWC}}{\rho_a} - \frac{\text{IWC}}{\rho_a}, \quad (\text{A15})$$

where  $w_{v,0}$  is the total mixing ratio in the parcel and LWC and IWC are the liquid and ice water content, respectively.

## A2. Binning Method for Ice Crystals

[66] The hybrid Lagrangian/Eulerian framework used to create and track drop and ice crystal bins is based on principles described by *Cooper et al.* [1997]. The parcel is initiated with a specified number of ice crystal bins, but with no sizes assigned to the bins. In the first time step that ice crystals are nucleated, their number concentrations and initial sizes are assigned to a size bin (equal to the size of the haze/droplet that freezes) in the hybrid framework and then grown in subsequent time steps. Ice particles created in subsequent time steps are either assigned to an existing crystal bin or to a new crystal bin if the newly created ice particles are not within 50% of the size of an existing crystal bin. To maintain mass balance when new ice crystals are

added to an existing crystal bin, the size associated with the existing crystal bin is redefined on the basis of the average mass of all crystals in that bin. To minimize needed bins, two bins that are close in size are merged if the sizes are less than 5% apart. A new crystal bin is also defined if the two neighboring sizes are more than 100% apart [*Cooper et al.*, 1997]. The size value assigned to the empty bins grows in time along with the bins that already have ice crystals in them.

## Appendix B: Heterogeneous Ice Nucleation Parameterizations

[67] Here we include the main equations to calculate heterogeneous ice nucleation with the parameterizations used in this study. The DW04 parameterization assumes the freezing rate ( $dN_f/dt$ ) of pure water droplets containing insoluble species can be computed from

$$-\frac{dN_f}{dt} = \frac{dN_u}{dt} = N_u a B_{h,i} V_d \exp(-a(273.15 - T)) \frac{dT}{dt} \quad (\text{B1})$$

for the immersion mode. Here  $N_u$  is the number of unfrozen droplets,  $V_d$  the droplet volume and  $a = 1^\circ\text{C}$  is a constant. The parameter  $B_{h,i}$  is the ice-nucleating efficiency in the immersion mode, and is unique for the different types of insoluble particles serving as IN (see DW04 for the values). For droplets containing soluble material, a freezing point depression is accounted for through the parameterization by *Koop et al.* [2000] (see DW04 for details).

[68] According to the PDA08 parameterization, the number of IN (in units of number of IN per kg of air) capable of forming ice crystals ( $n_{IN,X}$ ) as a function of temperature and ice saturation ratio in the immersion, condensation and deposition modes can be empirically expressed as

$$n_{IN,X} = \int_{\log[0.1\mu\text{m}]}^{\infty} (1 - \exp[-\mu_X(D_X, S_i, T)]) \frac{dn_X}{d \log D_X} d \log D_X, \quad (\text{B2})$$

where  $\mu_X$ , the average activated IN per aerosol of size  $D_X$ , is defined as

$$\mu_X = \alpha_X H_X(S_{i,v}, T) \xi(T) \left( \frac{n_{IN,1,*}(T, S_{i,v})}{\Omega_{X,1,*}} \right) \cdot \frac{d\Omega_X}{dn_X}. \quad (\text{B3})$$

The number of ice crystals nucleated for a given temperature and ice saturation ratio is scaled to a reference particle surface area  $\Omega_{X,1,*}$ . The value for the surface area is calculated for particles with diameter between 0.1 and 1  $\mu\text{m}$  from measurements during INSPECT I [*DeMott et al.*, 2003a; *Richardson et al.*, 2007] and is given by *Phillips et al.* [2008]. The term  $\Omega_X$  is the surface area for all particles  $>0.1 \mu\text{m}$  from the input size distribution in the simulations and  $d\Omega_X/dn_X \approx \pi D_X^2$ . The reference particle surface area ( $\Omega_{X,1,*}$ ) ensures that if  $\Omega_X > \Omega_{X,1,*}$ , more IN are active than measured during INSPECT I, and vice versa if  $\Omega_X < \Omega_{X,1,*}$ . The index  $X$  indicates the type of IN (i.e., dust, soot or bacteria). The term  $n_{IN,1,*}(T, S_{i,v})$  is the number of IN smaller than 1  $\mu\text{m}$ , as a function of temperature and ice saturation ratio, and is fitted to

the INSPECT data sets. The prefactor  $\xi$  ensures that no droplets freeze above  $-2^\circ\text{C}$ . Above  $-2^\circ\text{C}$ ,  $\xi = 0$ , while between  $-2$  and  $-5^\circ\text{C}$ ,  $\xi$  goes from 0 to unity with a cubic interpolation. The factor  $H_X$  ensures that only a fraction of the available IN can activate at water subsaturated conditions (based on laboratory observations), depending on temperature and ice supersaturation, while  $H_X = 1$  at water saturation. Finally,  $\alpha_X$  is the fractional contribution from aerosol group  $X$  to the measured IN concentration. The equations for the individual terms in equations (B2) and (B3) and more detailed descriptions can be found in the work of Phillips *et al.* [2008].

[69] The KC04 scheme is based on classical heterogeneous nucleation theory, but with allowance for deliquescent CCN to freeze. The germ rate formation of particles, per unit time, follows Pruppacher and Klett [1997] as

$$J_{s,fr}(T, r_N) \approx \frac{kT}{h} c_{l,s} 4\pi r_N^2 \exp\left[-\frac{\Delta F_{act}}{kT} - \frac{\Delta F_{cr}}{kT}\right]. \quad (\text{B4})$$

Here  $\Delta F_{act}$  is the activation energy at the solution-ice interface,  $\Delta F_{cr}$  the critical germ formation,  $k$  is the Boltzmann's constant,  $h$  is the Planck's constant,  $r_N$  the radius of the insoluble particle and  $c_{l,s}$  is the concentration of water molecules adsorbed on  $1\text{ cm}^{-2}$  of a surface. The critical free energy of germ formation is given as

$$\Delta F_{cr} = \frac{4}{3} \pi \sigma_{i/s} r_{cr}^2 f(m_{i/s}, r_{IN}, r_{cr}) - \alpha r_N^2 (1 - m_{is}) \sigma_{i/s}. \quad (\text{B5})$$

Here  $\sigma_{i/s}$  is the surface tension of the interface between the solution and ice. The function  $f(m_{is}, x)$  represents a geometric factor which takes into account the geometry of a spherical cap on a spherical particle, where  $m_{is} = \cos(\theta)$ . See KC04 or the work of Pruppacher and Klett [1997] for the form of  $f(m_{is}, x)$ . Finally,  $r_{cr}$  is the critical radius of an ice germ and follows KC04:

$$r_{cr} = \frac{2\sigma_{i/s}}{\rho_l I_m^{ef}(T) \ln\left(\frac{T_0}{T}\right) + \frac{RT\rho_l}{M_w} H_{cs} - C_\varepsilon \varepsilon^2 - \frac{2\sigma_{s/a}}{r_d}}, \quad (\text{B6})$$

where,  $T_0 = 273.15$ ,  $I_m^{ef}$  is the effective average latent heat of melting (see KC04),  $\varepsilon$  is the elastic strain,  $C_\varepsilon$  is a constant associated with the elastic strain and  $r_d$  is the radius of the droplet. The term  $H_{cs}$  is the logarithm of saturation ratio over an aqueous solution and is given by Köhler theory. Here we use the parameterization from equation (A3) to calculate  $H_{cs}$ :

$$H_{cs} = \ln(S) = \ln\left(\frac{D^3 - D_{dry}^3}{D^3 - D_{dry}^3(1 - \kappa)} \exp\left(\frac{4\sigma_{s/a} M_w}{RT\rho_w D}\right)\right). \quad (\text{B7})$$

See KC04 for more detailed discussion of their parameterization.

[70] **Acknowledgments.** This work has been supported by the National Science Foundation (NSF) Science and Technology Center for Multi-Scale Modeling of Atmospheric Processes, managed by Colorado State University under cooperative agreement ATM-0425247, NSF grant ATM-0611936, and by the NASA MAP (Modeling and Analysis Program) NNG06GB60G. We thank Vitaly Khvorostyanov for sharing his ice nucleation code. We also thank three anonymous reviewers for providing comments that improved the paper.

## References

Bergeron, T. (1935), On the physics of clouds and precipitation, paper presented at 5th Assembly U.G.G.I., Lisbon, vol. 2, pp. 156–178.

- Brown, P. N., G. D. Byrne, and A. C. Hindmarsh (1989), Vode—A variable-coefficient ODE Solver, *SIAM J. Sci. Stat. Comput.*, *10*(5), 1038–1051.
- Cooper, W. A. (1986), Ice initiation in natural clouds, in *Precipitation Enhancement—A Scientific Challenge*, Meteorol. Monogr., vol. 21, edited by R. G. Braham Jr., pp. 29–32, Am. Meteorol. Soc., Boston, Mass.
- Cooper, W. A., and G. Vali (1981), The origin of ice in mountain cap clouds, *J. Atmos. Sci.*, *38*(6), 1244–1259.
- Cooper, W. A., R. T. Bruintjes, and G. K. Mather (1997), Calculations pertaining to hygroscopic seeding with flares, *J. Appl. Meteorol.*, *36*(11), 1449–1469.
- DeMott, P. J. (1990), An exploratory study of ice nucleation by soot aerosols, *J. Appl. Meteorol.*, *29*(10), 1072–1079.
- DeMott, P. J. (2002), Laboratory studies of cirrus cloud processes, in *Cirrus*, edited by D. K. Lynch *et al.*, pp. 102–135, Oxford Univ. Press, New York.
- DeMott, P. J., D. C. Rogers, and S. M. Kreidenweis (1997), The susceptibility of ice formation in upper tropospheric clouds to insoluble aerosol components, *J. Geophys. Res.*, *102*(D16), 19,575–19,584.
- DeMott, P. J., D. C. Rogers, S. M. Kreidenweis, Y. L. Chen, C. H. Twohy, D. Baumgardner, A. J. Heymsfield, and K. R. Chan (1998), The role of heterogeneous freezing nucleation in upper tropospheric clouds: Inferences from SUCCESS, *Geophys. Res. Lett.*, *25*(9), 1387–1390.
- DeMott, P. J., D. J. Cziczo, A. J. Prenni, D. M. Murphy, S. M. Kreidenweis, D. S. Thomson, R. Borys, and D. C. Rogers (2003a), Measurements of the concentration and composition of nuclei for cirrus formation, *Proc. Natl. Acad. Sci. U. S. A.*, *100*(25), 14,655–14,660.
- DeMott, P. J., K. Sassen, M. R. Poellot, D. Baumgardner, D. C. Rogers, S. D. Brooks, A. J. Prenni, and S. M. Kreidenweis (2003b), African dust aerosols as atmospheric ice nuclei, *Geophys. Res. Lett.*, *30*(14), 1732, doi:10.1029/2003GL017410.
- DeMott, P. J., *et al.* (2008), The Fourth International Ice Nucleation Workshop (ICIS 2007): Objectives and preliminary results, paper presented at 15th International Conference on Clouds and Precipitation, Cancun, Mexico.
- Diehl, K., and S. Wurzler (2004), Heterogeneous drop freezing in the immersion mode: Model calculations considering soluble and insoluble particles in the drops, *J. Atmos. Sci.*, *61*(16), 2063–2072.
- Diehl, K., M. Simmel, and S. Wurzler (2006), Numerical sensitivity studies on the impact of aerosol properties and drop freezing modes on the glaciation, microphysics, and dynamics of clouds, *J. Geophys. Res.*, *111*, D07202, doi:10.1029/2005JD005884.
- Diehl, K., M. Simmel, and S. Wurzler (2007), Effects of drop freezing on microphysics of an ascending cloud parcel under biomass burning conditions, *Atmos. Environ.*, *41*(2), 303–314.
- Dusek, U., G. P. Reischl, and R. Hitznerberger (2006), CCN activation of pure and coated carbon black particles, *Environ. Sci. Technol.*, *40*(4), 1223–1230.
- Ervens, B., G. Feingold, and S. M. Kreidenweis (2005), Influence of water-soluble organic carbon on cloud drop number concentration, *J. Geophys. Res.*, *110*, D18211, doi:10.1029/2004JD005634.
- Feingold, G., and A. J. Heymsfield (1992), Parameterizations of condensational growth of droplets for use in General-Circulation Models, *J. Atmos. Sci.*, *49*(23), 2325–2342.
- Feingold, G., and S. Kreidenweis (2000), Does cloud processing of aerosol enhance droplet concentrations?, *J. Geophys. Res.*, *105*(D19), 24,351–24,361.
- Feingold, G., S. M. Kreidenweis, and Y. P. Zhang (1998), Stratocumulus processing of gases and cloud condensation nuclei: 1. Trajectory ensemble model, *J. Geophys. Res.*, *103*(D16), 19,527–19,542.
- Field, P. R., O. Mohler, P. Connolly, M. Kramer, R. Cotton, A. J. Heymsfield, H. Saathoff, and M. Schnaiter (2006), Some ice nucleation characteristics of Asian and Saharan desert dust, *Atmos. Chem. Phys.*, *6*, 2991–3006.
- Findeisen, W. (1938), Kolloid-meteorologische Vorgänge bei der Neiderschlagsbildung, *Meteorol. Z.*, *55*, 121–133.
- Fletcher, N. H. (1962), *The Physics of Rain Clouds*, 386 pp., Cambridge Univ. Press, New York.
- Fletcher, N. H. (1969), Active sites and ice crystal nucleation, *J. Atmos. Sci.*, *26*(6), 1266–1278.
- Gierens, K. (2003), On the transition between heterogeneous and homogeneous freezing, *Atmos. Chem. Phys.*, *3*, 437–446.
- Haag, W., and B. Kärcher (2004), The impact of aerosols and gravity waves on cirrus clouds at midlatitudes, *J. Geophys. Res.*, *109*, D12202, doi:10.1029/2004JD004579.
- Heymsfield, A. J., and L. M. Miloshevich (1993), Homogeneous ice nucleation and supercooled liquid water in orographic wave clouds, *J. Atmos. Sci.*, *50*, 2335–2353.
- Hobbs, P. V., and A. L. Rangno (1990), Rapid development of high ice particle concentrations in small polar maritime cumuliform cloud, *J. Atmos. Sci.*, *47*, 2710–2722.
- Jensen, E. J., L. Pfister, A. S. Ackerman, A. Tabazadeh, and O. B. Toon (2001), A conceptual model of the dehydration of air due to freeze-drying

- by optically thin, laminar cirrus rising slowly across the tropical tropopause, *J. Geophys. Res.*, *106*(D15), 17,237–17,252.
- Kärcher, B. (2003), Simulating gas-aerosol-cirrus interactions: Process-oriented microphysical model and applications, *Atmos. Chem. Phys.*, *3*, 1645–1664.
- Kärcher, B., and U. Lohmann (2003), A parameterization of cirrus cloud formation: Heterogeneous freezing, *J. Geophys. Res.*, *108*(D15), 4402, doi:10.1029/2002JD003136.
- Kärcher, B., T. Peter, U. M. Biermann, and U. Schumann (1996), The initial composition of jet condensation trails, *J. Atmos. Sci.*, *53*(21), 3066–3083.
- Kärcher, B., J. Hendricks, and U. Lohmann (2006), Physically based parameterization of cirrus cloud formation for use in global atmospheric models, *J. Geophys. Res.*, *111*, D01205, doi:10.1029/2005JD006219.
- Kärcher, B., O. Möhler, P. J. DeMott, S. Pechtl, and F. Yu (2007), Insights into the role of soot aerosols in cirrus cloud formation, *Atmos. Chem. Phys.*, *7*(16), 4203–4227.
- Khvorostyanov, V. I., and J. A. Curry (2000), A new theory of heterogeneous ice nucleation for application in cloud and climate models, *Geophys. Res. Lett.*, *27*, 4081–4084.
- Khvorostyanov, V. I., and J. A. Curry (2004), The theory of ice nucleation by heterogeneous freezing of deliquescent mixed CCN. part I: Critical radius, energy, and nucleation rate, *J. Atmos. Sci.*, *61*(22), 2676–2691.
- Khvorostyanov, V. I., and J. A. Curry (2005), The theory of ice nucleation by heterogeneous freezing of deliquescent mixed CCN. part II: Parcel model simulation, *J. Atmos. Sci.*, *62*(2), 261–285.
- Khvorostyanov, V. I., H. Morrison, J. A. Curry, D. Baumgardner, and P. Lawson (2006), High supersaturation and modes of ice nucleation in thin tropopause cirrus: Simulation of the 13 July 2002 Cirrus Regional Study of Tropical Anvils and Cirrus Layers case, *J. Geophys. Res.*, *111*, D02201, doi:10.1029/2004JD005235.
- Koehler, K. (2007), The impact of natural dust aerosol on warm and cold cloud formation, Dissertation thesis, Colo. State Univ., Fort Collins.
- Koehler, K. A., S. M. Kreidenweis, P. J. DeMott, A. J. Prenni, C. M. Carrico, B. Ervens, and G. Feingold (2006), Water activity and activation diameters from hygroscopicity data. part II: Application to organic species, *Atmos. Chem. Phys.*, *6*, 795–809.
- Koehler, K. A., S. M. Kreidenweis, P. J. DeMott, A. J. Prenni, and M. D. Petters (2007), Potential impact of Owens (dry) Lake dust on warm and cold cloud formation, *J. Geophys. Res.*, *112*, D12210, doi:10.1029/2007JD008413.
- Koop, T., B. P. Luo, A. Tsias, and T. Peter (2000), Water activity as the determinant for homogeneous ice nucleation in aqueous solutions, *Nature*, *406*(6796), 611–614.
- Langham, E. J., and B. J. Mason (1958), The Heterogeneous and Homogeneous Nucleation of Supercooled Water, *Proc. R. Soc. London Ser. A*, *247*(1251), 493–504.
- Lin, R. F., D. O. Starr, P. J. DeMott, R. Cotton, K. Sassen, E. Jensen, B. Kärcher, and X. H. Liu (2002), Cirrus Parcel Model Comparison Project. Phase 1: The critical components to simulate cirrus initiation explicitly, *J. Atmos. Sci.*, *59*(15), 2305–2329.
- Liu, X. H., and J. E. Penner (2005), Ice nucleation parameterization for global models, *Meteorol. Z.*, *14*(4), 499–514.
- Liu, X., J. E. Penner, S. J. Ghan, and M. Wang (2007), Inclusion of ice microphysics in the NCAR community atmospheric model version 3 (CAM3), *J. Clim.*, *20*(18), 4526–4547.
- Lohmann, U., and K. Diehl (2006), Sensitivity studies of the importance of dust ice nuclei for the indirect aerosol effect on stratiform mixed-phase clouds, *J. Atmos. Sci.*, *63*(3), 968–982.
- Lohmann, U., P. Stier, C. Hoese, S. Ferrachat, S. Kloster, E. Roeckner, and J. Zhang (2007), Cloud microphysics and aerosol indirect effects in the global climate model ECHAM5-HAM, *Atmos. Chem. Phys.*, *7*, 3425–3446.
- Marcollì, C., S. Gedamke, T. Peter, and B. Zobrist (2007), Efficiency of immersion mode ice nucleation on surrogates of mineral dust, *Atmos. Chem. Phys.*, *7*(19), 5081–5091.
- Meyers, M. P., P. J. DeMott, and W. R. Cotton (1992), New primary ice-nucleation parameterizations in an explicit cloud model, *J. Appl. Meteorol.*, *31*(7), 708–721.
- Möhler, O., et al. (2006), Efficiency of the deposition mode ice nucleation on mineral dust particles, *Atmos. Chem. Phys.*, *6*, 3007–3021.
- Möhler, O., P. J. DeMott, G. Vali, and Z. Levin (2007), Microbiology and atmospheric processes: The role of biological particles in cloud physics, *Biogeosciences*, *4*(6), 1059–1071.
- Morrison, H., and J. O. Pinto (2006), Intercomparison of bulk cloud microphysics schemes in mesoscale simulations of springtime Arctic mixed-phase stratiform clouds, *Mon. Weather Rev.*, *134*(7), 1880–1900.
- Petters, M. D., and S. M. Kreidenweis (2007), A single parameter representation of hygroscopic growth and cloud condensation nucleus activity, *Atmos. Chem. Phys.*, *7*, 1961–1971.
- Phillips, V. T. J., P. J. DeMott, and C. Andronache (2008), An empirical parameterization of heterogeneous ice nucleation for multiple chemical species of aerosol, *J. Aerosol Sci.*, *65*, 2757–2783, doi:10.1175/2007JAS2546.1.
- Popovicheva, O. B., N. M. Persiantseva, E. E. Lukhovitskaya, N. K. Shonija, N. A. Zubareva, B. Demirdjian, D. Ferry, and J. Suzanne (2004), Aircraft engine soot as contrail nuclei, *Geophys. Res. Lett.*, *31*, L11104, doi:10.1029/2003GL018888.
- Prenni, A. J., P. J. DeMott, C. Twohy, M. R. Poellot, S. M. Kreidenweis, D. C. Rogers, S. D. Brooks, M. S. Richardson, and A. J. Heymsfield (2007a), Examinations of ice formation processes in Florida cumuli using ice nuclei measurements of anvil ice crystal particle residues, *J. Geophys. Res.*, *112*, D10221, doi:10.1029/2006JD007549.
- Prenni, A. J., J. Y. Harrington, M. Tjernstrom, P. J. DeMott, A. Avramov, C. N. Long, S. M. Kreidenweis, P. Q. Olsson, and J. Verlinde (2007b), Can ice-nucleating aerosols affect arctic seasonal climate?, *Bull. Am. Meteorol. Soc.*, *88*(4), 541–550.
- Pruppacher, H. R., and J. D. Klett (1997), *Microphysics of Clouds and Precipitation*, 2nd rev. ed., 954 pp., Springer, New York.
- Rangno, A. L., and P. V. Hobbs (1991), Ice particle concentrations and precipitation development in small polar maritime cumuliform clouds, *Q. J. R. Meteorol. Soc.*, *117*, 207–241.
- Richardson, M. S., et al. (2007), Measurements of heterogeneous ice nuclei in the western United States in springtime and their relation to aerosol characteristics, *J. Geophys. Res.*, *112*, D02209, doi:10.1029/2006JD007500.
- Rogers, D. C. (1998), Development of a continuous flow thermal gradient diffusion chamber for ice nucleation studies, *Atmos. Res.*, *22*, 149–181.
- Sassen, K., and G. C. Dodd (1988), Homogeneous nucleation rate for highly supercooled cirrus cloud droplets, *J. Atmos. Sci.*, *45*(8), 1357–1369.
- Sassen, K., and V. I. Khvorostyanov (2007), Microphysical and radiative properties of mixed-phased altocumulus: A model evaluation of glaciation effects, *Atmos. Res.*, *84*, 390–398.
- Sassen, K., P. J. DeMott, J. M. Prospero, and M. R. Poellot (2003), Saharan dust storms and indirect aerosol effects on clouds: CRYSTAL-FACE results, *Geophys. Res. Lett.*, *30*(12), 1633, doi:10.1029/2003GL017371.
- Shaw, R. A., A. J. Durant, and Y. Mi (2005), Heterogeneous surface crystallization observed in undercooled water, *J. Phys. Chem. B*, *109*(20), 9865–9868.
- Stith, J. L., et al. (2009), An overview of aircraft observations from the Pacific Dust Experiment campaign, *J. Geophys. Res.*, *114*, D05207, doi:10.1029/2008JD010924.
- Stokes, R. H., and R. A. Robinson (1966), Interactions in aqueous nonelectrolyte solutions. I: Solute-solvent equilibria, *J. Phys. Chem.*, *70*(7), 2126–2131.
- Storelvmo, T., J. E. Kristjansson, and U. Lohmann (2008), Aerosol influence on mixed-phase clouds in CAM-Oslo, *J. Atmos. Sci.*, *65*, 3214–3230, doi:10.1175/2008JAS2430.1.
- Turnbull, D., and B. Vonnegut (1952), Nucleation catalysis, *Ind. Eng. Chem.*, *44*(6), 1292–1298.
- Vali, G. (1985), Nucleation terminology, *Bull. Am. Meteorol. Soc.*, *66*(11), 1426–1427.
- Vali, G. (1994), Freezing rate due to heterogeneous nucleation, *J. Atmos. Sci.*, *51*(13), 1843–1856.
- Vali, G. (2008), Repeatability and randomness in heterogeneous freezing nucleation, *Atmos. Chem. Phys.*, *8*, 5017–5031.
- Wegener, A. (1911), *Thermodynamik der Atmosphäre*, Verlag Von Johann Ambrosius Barth, Leipzig.

P. J. DeMott and S. M. Kreidenweis, Department of Atmospheric Science, Colorado State University, 1371 Campus Delivery, Fort Collins, CO 80523-1371, USA.

T. Eidhammer, National Center for Atmospheric Research, 1850 Table Mesa Drive, Boulder, CO 80305, USA. (trude@ucar.edu)